Liquid Crystals
Publication details, including instructions for authors and subscription information:
http://www.informaworld.com/smpp/title~content=t713926090

A comparison of proton-detected ^{13}C local field experiments with deuterium NMR at natural abundance for studying liquid crystals

James W. Emsley[a]; Philippe Lesot[b]; Giuseppina De Luca[c]; Anne Lesage[d]; Denis Merlet[b]; Giuseppe Pileio[a]
[a] School of Chemistry, University of Southampton, Southampton SO17 1BJ, UK [b] Laboratoire de Chimie Structurale Organique, RMN en Milieu Orienté, Université de Paris-Sud (XI), ICMMO, UMR CNRS 8182, F-91405 Orsay cedex, France [c] Dipartimento di Chimica, Universita della Calabria, 87030 Arcavacata di Rende, Italy [d] Université de Lyon, Laboratoire de Chimie, Ecole Normale Supérieure de Lyon, CNRS, France

To cite this Article Emsley, James W. , Lesot, Philippe , De Luca, Giuseppina , Lesage, Anne , Merlet, Denis and Pileio, Giuseppe(2008) 'A comparison of proton-detected ^{13}C local field experiments with deuterium NMR at natural abundance for studying liquid crystals', Liquid Crystals, 35: 4, 443 — 464
To link to this Article: DOI: 10.1080/02678290801935887
URL: http://dx.doi.org/10.1080/02678290801935887

Liquid Crystals,
Vol. 35, No. 4, April 2008, 443–464

Taylor & Francis
Taylor & Francis Group

A comparison of proton-detected ^{13}C local field experiments with deuterium NMR at natural abundance for studying liquid crystals

James W. Emsley[a]*, Philippe Lesot[b], Giuseppina De Luca[c], Anne Lesage[d], Denis Merlet[b] and Giuseppe Pileio[a]

[a]*School of Chemistry, University of Southampton, Southampton SO17 1BJ, UK;* [b]*Laboratoire de Chimie Structurale Organique, RMN en Milieu Orienté, Université de Paris-Sud (XI), ICMMO, UMR CNRS 8182, Bât. 410, F-91405 Orsay cedex, France;* [c]*Dipartimento di Chimica, Universita della Calabria, 87030 Arcavacata di Rende, Italy;* [d]*Université de Lyon, Laboratoire de Chimie, Ecole Normale Supérieure de Lyon, CNRS, France*

(Received 23 November 2007; accepted 22 January 2008)

A comparison is made between the information which can be derived on structure, conformation and orientational order of the molecules in a nematic liquid crystal 4-pentyl-4′-cyanobiphenyl (5CB) from the NMR spectra of the deuterium atoms at natural abundance (NAD NMR), and the two-dimensional proton-detected ^{13}C local field experiment (PDLF). The nine residual quadrupolar splittings, $\Delta\nu_k$, obtained experimentally have been compared with quadrupolar tensors and a geometry and conformational potentials calculated by the DFT method B3LYP/6-311G**. The PDLF experiment yielded 42 scaled ^{13}C–^{1}H residual dipolar couplings, kD_{CiHj}. The scaling factor, k, is determined experimentally by comparing unscaled and scaled residual dipolar couplings in a sample of fluorobenzene dissolved in a nematic liquid crystalline solvent. The corrected residual dipolar couplings, D_{CiHj}, are used to investigate the structure and rotational potentials about each bond in the molecule.

Keywords: proton-detected ^{13}C local field experiment; deuterium NMR at natural abundance

1. Introduction

The first studies of liquid crystals by NMR that yielded sufficient data to investigate their structure, conformation and orientational order used deuterium NMR of deuterium-enriched samples (*1, 2*). This continues to be a popular method, but it has the considerable disadvantage that deuterated samples have to be prepared, and this has restricted the application of this method. The data obtained, which is usually the residual quadrupolar splittings, $\Delta\nu_k$, at the deuterated sites, has proved to be very useful in testing theories of orientational order, particularly of flexible mesogens, and also to follow changes in phase. The availability of deuterated samples made possible the measurement of relaxation rates, including individual spectral densities, for the deuterium nuclei at different sites in the molecule (*3–6*). There were also early studies of the NMR spectra of ^{13}C at natural abundance. These experiments used proton decoupling to give single resonance lines for each set of non-equivalent ^{13}C nuclei in a mesogen, but the information content of the spectra is low, being just the chemical shift anisotropies (*2*). A significant improvement was made by Fung *et al.* (*7, 8*) who introduced the two-dimensional (2D) separated-local field (SLF) ^{13}C experiment for studying liquid crystalline samples, which gives, for each resolved carbon-13 resonance, scaled heteronuclear dipolar couplings with ^{1}H nuclei in close proximity. This experiment suffers from the disadvantage of dipolar doublets becoming unresolved in the indirect spectral dimension because of longer-range couplings. However, this problem was largely solved by the development of the 2D proton-detected ^{13}C local field experiment (PDLF) (*9, 10*). Both the SLF and PDLF experiments require high power proton decoupling, and this can not be achieved with the radio-frequency (RF) field strength available on standard liquids NMR spectrometers. Recent technical developments have made the PDLF and deuterium NMR experiments much easier to apply, and they are poised to be the method of choice for obtaining detailed structural and orientation information on molecules which form liquid crystal phases. The most important advance is the availability of spectrometers designed to study solid samples, which have more than adequate proton decoupling power to give resolved resonances on static liquid crystalline samples. These spectrometers, together with the increased sensitivity gained by using a high field can also provide deuterium spectra on un-enriched (natural abundance deuterium, NAD NMR) samples (*11*). A second development is the availability of probes with receiver coils and preamplifiers cooled to very low temperatures by helium gas for high resolution, liquids spectrometers, and which are tuned to deuterium. These probes have so far been used only for liquid crystalline samples having relatively low

*Corresponding author. Email: jwe@soton.ac.uk

ISSN 0267-8292 print/ISSN 1366-5855 online

DOI: 10.1080/02678290801935887
http://www.informaworld.com

orientational order, and here we explore their use for strongly ordered samples.

The residual quadrupolar splittings measured from NAD NMR spectra, and the scaled ^{13}C–^{1}H residual dipolar couplings from PDLF ^{13}C spectra have very similar, but not entirely equivalent, information content. Their use in investigating orientational order and conformational distributions presents different challenges.

Thus, the principal problem with the data from PDLF experiments is that the splittings observed in the indirect spectral dimension are related to scaled dipolar couplings, kD_{CH}, between ^{13}C and ^{1}H nuclei. The scaling factor k depends on the particular proton–proton homonuclear decoupling sequence and an experimental method for determining its value is described here which consists in recording a PDLF ^{13}C spectrum on a sample containing a solute. The criterion for choosing an appropriate solute is that it should have a ^{1}H spectrum that can be analysed to yield the dipolar couplings between all the interacting nuclei, including those to the ^{13}C nuclei. Comparison of these couplings with those observed in the PDLF ^{13}C spectrum will enable the determination of the value of k. The solute chosen is fluorobenzene, which gives well-resolved ^{1}H and ^{19}F spectra when dissolved in a liquid crystalline solvent, and which yields both ^{1}H–^{13}C and ^{19}F–^{13}C dipolar couplings.

The main problem with the NAD NMR experiment is that it yields residual quadrupolar splittings, $\Delta\nu_k$, for each deuterium site in the molecule, but it does not provide an assignment of these peaks to position, nor does it contain information on their signs. There is a similar assignment problem for the PDLF ^{13}C NMR spectra, and it will be demonstrated that comparing NAD NMR and PDLF ^{13}C spectra may help in the assignment of both types of spectra. This is illustrated here by the results of NAD NMR and PDLF ^{13}C experiments on samples of the nematogen 4-pentyl-4′-cyanobiphenyl (5CB).

Having obtained values and signs of $\Delta\nu_k$ and D_{CH} their interpretation in terms of the structure, conformation and orientational order presents extra challenges. For both kinds of data sets there is often insufficient information to determine the structure of the molecule, particularly that of alkyl chains. In earlier studies the structural parameters, bond lengths and angles, were either taken from studies of crystal structures, or assumed to have values obtained experimentally for similar compounds. A more general approach, demonstrated here, is to perform a quantum chemical calculation on a single molecule as providing good estimates of the geometrical parameters. These same calculations can also give good guidelines on the conformational distributions expected for the molecules in the liquid crystalline state.

The observed residual quadrupolar splittings, $\Delta\nu_k$, are related to the values of quadrupolar coupling tensors, $\boldsymbol{q}_k$, whose magnitudes and orientation have usually been estimated by reference to experimental determinations of these for similar molecules. Here, we demonstrate that quantum chemical calculations provide a good way of estimating these values.

2. Experimental

Two-dimensional PDLF experiments

Figure 1 shows the pulse sequence for the PDLF experiment employed here.

The 2D PDLF spectra of 5CB in the nematic phase, and of a sample of fluorobenzene dissolved in the nematic solvent ZLI 1695 were acquired on a narrow bore 700 MHz (proton frequency) Avance Bruker spectrometer equipped with a double resonance 4 mm cross-polarization magic angle spinning (CPMAS) solid-state NMR probe (coil oriented at 54.7°). The benefit of this equipment is the availability of high RF decoupling powers. The (static) samples were contained in 4 mm rotors (sample volume 92 µl). The contact time of the CP step was 1.5 ms. A ramped RF field centred at 75 kHz was applied on protons, while the carbon RF field was matched to obtain optimal signal. SPINAL-64 (*13*) heteronuclear decoupling was applied during ^{13}C acquisition with a proton nutation frequency $\nu_1 = 50$ kHz. Quadrature detection in the F_1 dimension was achieved using the States method (*14*) on the proton CP pulse. During the indirect detection time t_1, DUMBO-1 proton homonuclear decoupling (*12*) was implemented with a radio-frequency field strength of $\nu_1 = 50$ kHz. Each decoupling cycle ($\tau_C = 60$ µs) was divided into 60 phase steps of 1 µs

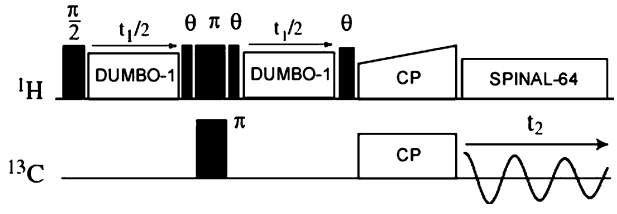

Figure 1. Pulse sequence for the two-dimensional PDLF experiment. The continuously phase-modulated DUMBO-1 homonuclear decoupling sequence (*12*) is applied during the indirect evolution time t_1 to suppress the proton–proton dipolar couplings, whereas the heteronuclear decoupling sequence SPINAL-64 (*13*) is applied in t_2.

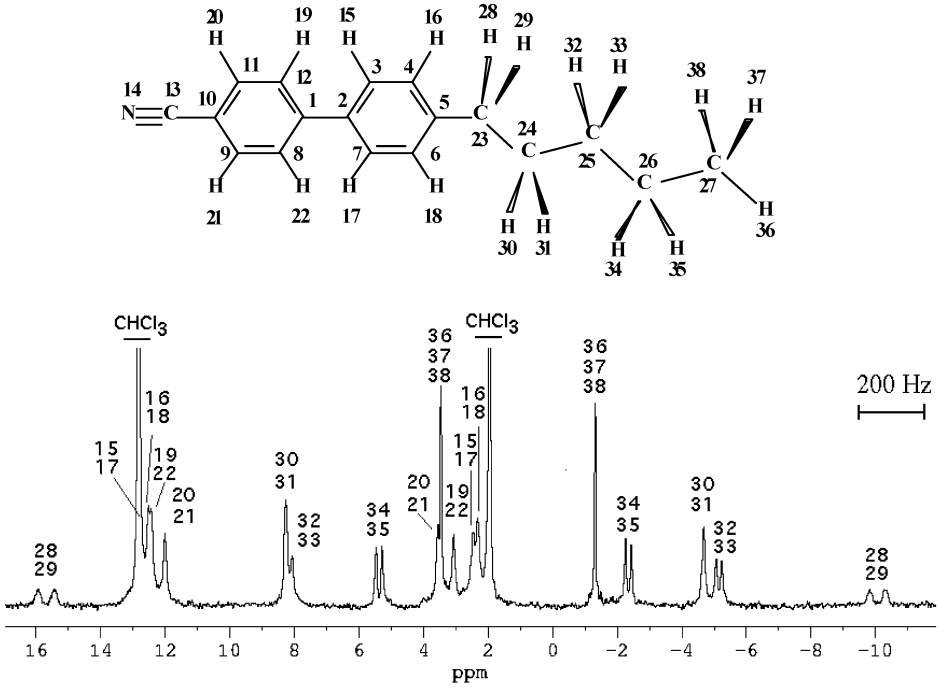

Figure 2. 92 MHz ^{2}H–{^{1}H} 1D spectrum of 5CB dissolved in the PBLG/$CHCl_3$ mesophase at 300 K. The spectrum is the result of accumulating 35k free-induction decays of 3k data points, and zero filling to 64k. Protons were decoupled using the Waltz-16 sequence. Fourier transformation was performed without prior application of a window function. The total recording time was 2 h. The assignment of doublets, based on the ^{2}H chemical shifts, was facilitated by recording a NAD Q-COSY 2D spectrum (*16, 17*).

each. The overall phase of DUMBO-1 decoupling was adjusted to make the effective decoupling field lie in the (x, z) plane. The short θ pulses (1 μs) rotate magnetization back into the (x, y) plane from the evolution plane perpendicular to the decoupling field (and towards for the "$-\theta$" pulses). The 180° pulse lengths on proton and carbon were set respectively to 10 μs and 8.7 μs. An 8-step phase cycle was used to select the proper coherence pathway (pulse program available upon request to the authors). Other experimental details are given in figure captions.

One-dimensional spectra of fluorobenzene

High resolution 1D proton and fluorine-19 spectra of fluorobenzene dissolved in the nematic solvent ZLI 1695 were obtained on a narrow bore Bruker Avance 500 MHz (proton frequency) spectrometer designed for liquid state samples, using standard 5 mm NMR glass tubes. A high signal-to-noise ratio was required in order to detect the ^{13}C satellite lines in these spectra.

A proton-decoupled ^{13}C spectrum was recorded on a sample contained in a 4 mm rotor on a Bruker 700 MHz (proton frequency) as described for the 2D PDLF experiments.

One-dimensional deuterium spectra

NAD spectra of 5CB were obtained in two ways: (i) on a narrow bore Bruker Avance 600 MHz (proton frequency) spectrometer using a cryogenic probe optimized for detection of deuterium NMR. The sample was contained in 5 mm NMR tube. (ii) On a narrow bore 700 MHz (proton frequency) Avance Bruker spectrometer equipped with a double resonance CPMAS solid-state NMR probe tuned to deuterium. The sample was contained in a 4 mm rotor (sample volume 92 μl).

3. Spectra of deuterium at natural abundance

Our first aim is to demonstrate the ease of obtaining a NAD spectrum of a liquid crystalline sample. When the liquid crystalline molecules have low orientational order, for example when a mesogen such as 5CB is dissolved in a polypeptide chiral nematic solvent comprising poly-γ-benzyl-L-glutamate (PBLG) (*15–17*) and chloroform, a ^{2}H–{^{1}H} spectrum with narrow lines can be obtained at 92.1 MHz using a 5 mm cryoprobe (*18*) tuned to deuterium, as shown in Figure 2.

The low orientational order means that the dipolar couplings between the deuterium and

hydrogen nuclei are small enough to be efficiently decoupled by the low proton decoupler power available with this probe, leading to narrow lines. Note that some of the peaks from the CD_2 groups in this spectrum consist of four lines rather than the two expected from 5CB. The extra splittings arise because of the interaction of this prochiral molecule with the chiral PBLG molecules (*19*).

When the 5CB molecules have high orientational order, as in the pure sample in the nematic phase, then the RF power required for efficient proton decoupling is insufficient using the cryoprobe. This is evident in the spectra obtained for 5CB at 295 K and 305 K, shown in Figures 3 (a) and 3 (b).

At the higher temperature the largest quadrupolar doublet is observed, but with very broad lines, and only three of the four expected aromatic splittings are seen. At the lower temperature the lines have broadened even more and the largest splitting is not observed.

Figure 3 (c) shows a ^2H–$\{^1H\}$ spectrum recorded at 107.47 MHz on a sample contained in a static, MAS rotor at 293 K. The MAS probe is designed for high power proton decoupling, and using a 50 kHz decoupling field removed the couplings to protons completely and leads to very narrow lines (90 to 130 Hz widths).

Assignment of the NAD spectrum of 5CB

The NAD 1D spectra in Figure 3 consist of a pair of lines from each of the nine groups of non-equivalent deuterium atoms. The pair of lines from the methyl group can be unambiguously assigned, based on their relative intensity. The chemical shifts of the other peaks clearly differentiate the four aliphatic CD_2 from the four equivalent pairs from the biphenyl group. The only unambiguous method for assigning the peaks is by synthesis of partially deuterated samples. This has been done only for certain positions for 5CB, leading to the unambiguous assignment of the peaks from deuteriums at positions 28 and 29. Other methods of assignment rely on an interpretation of the magnitudes of the residual quadrupolar splittings in terms of the structure and conformational distribution of the molecules. It has been suggested that the spin-lattice relaxation rates for the deuterium atoms in the chain for molecules like 5CB, which have a flexible alkyl chain attached to a more rigid aromatic part, should increase monotonically from positions 28,29 to the end methyl group (*5, 6*). This gives the assignment for the aliphatic positions shown in Table 1. To assign the peaks for deuteriums in the aromatic sites is more difficult, and involves examining the relationship between the residual quadrupolar splittings, $\Delta\nu_k$, at site k, and the structure and orientational order of the molecules. This is complicated for a non-rigid molecule such as 5CB by the effect of the intramolecular motion present by virtue of rotations about bonds. Thus, the residual quadrupolar splittings for a deuterium nucleus at the k^{th} site in the n^{th} rigid conformation are given by

$$\begin{aligned}\Delta\nu_k(n) = \frac{3}{4}q_{aa}(k,n)[&S_{zz}(n)\{(3\cos^2\theta_{azk}-1)\\ &+\eta(k,n)(\cos^2\theta_{bzk}-\cos^2\theta_{czk})\}\\ &+(S_{xx}(n)-S_{yy}(n))\{\cos^2\theta_{axk}-\cos^2\theta_{ayk}\\ &+\frac{1}{3}\eta(k,n)(\cos^2\theta_{bxk}-\cos^2\theta_{byk}\\ &-\cos^2\theta_{cxk}+\cos^2\theta_{cyk}\}\\ &+4S_{xy}(n)\{\cos\theta_{axk}\cos\theta_{ayk}\\ &+\frac{1}{3}\eta(k,n)(\cos\theta_{bxk}\cos\theta_{byk}\\ &-\cos\theta_{cxk}\cos\theta_{cyk})\}+4S_{xz}(n)\{\cos\theta_{axk}\cos\theta_{azk}\\ &+\frac{1}{3}\eta(k,n)(\cos\theta_{bxk}\cos\theta_{bzk}\\ &-\cos\theta_{cxk}\cos\theta_{zk})\}\\ &+4S_{yz}(n)\{\cos\theta_{ayk}\cos\theta_{azk}\\ &+\frac{1}{3}\eta(k,n)(\cos\theta_{byk}\cos\theta_{bzk}\\ &-\cos\theta_{cyk}\cos\theta_{czk})\}]\end{aligned} \quad (1)$$

where

$$\eta(k,n) = (q_{bb}(k,n)-q_{cc}(k,n))/q_{aa}(k,n) \quad (2)$$

and the $q_{\alpha\alpha}(k,n)$ are principal components of the quadrupolar tensor. The axes x, y, z are fixed in the molecule, and the $S_{xy}(n)$ etc. are elements of the Saupe order matrix for the molecule in the nth conformation. If the molecule is converting rapidly between all the allowed conformations then the observed splittings are averages given by

$$\Delta\nu_k = \sum_n \Delta\nu(k,n)P_{LC}(n), \quad (3)$$

where $P_{LC}(n)$ is the probability that the molecule is in one of a discrete set of conformations. To calculate the values of $\Delta\nu_k$ it is necessary in general to have a reasonable approximation for the values of all the parameters in Equations (1)–(3). These are of four types: (1) the bond lengths and angles, which may reasonably be assumed

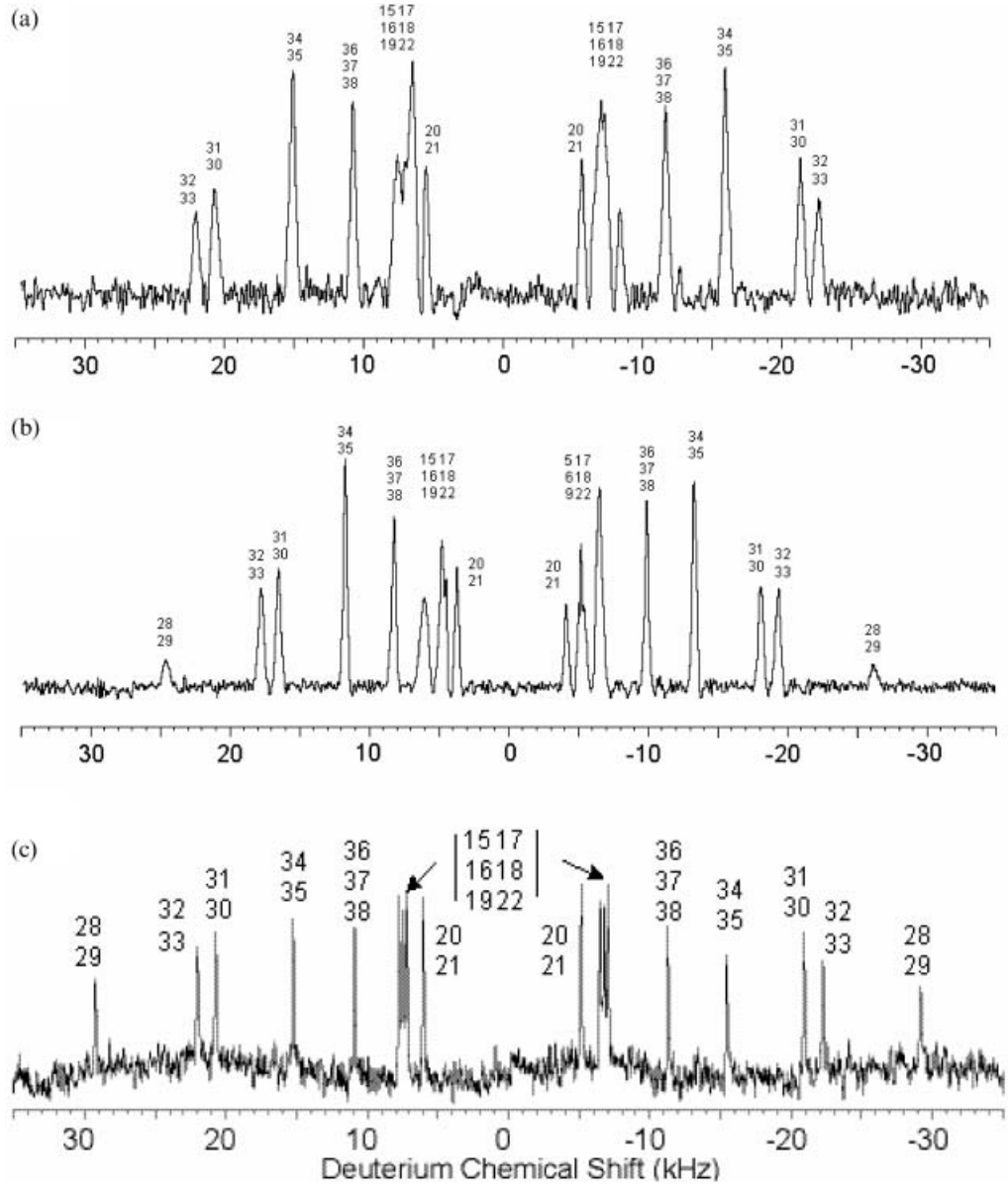

Figure 3. (a, b) The 92 MHz ^{2}H–{^{1}H} spectra recorded using a cryogenic probe of 5CB in the nematic phase at 305 and 295 K, respectively. Both spectra are the result of accumulating 100k free-induction decays of 3k data points, and zero filling to 64k. Fourier transformation was performed without prior application of a window function. A trapezoidal window was applied prior to Fourier transformation, followed by a baseline correction. In both (a) and (b), the decoupler was active only during the acquisition time of 0.08 s for (a) and 0.4 s for (b), and there was a 0.2 s (a) and 0.1 s (b) delay between pulses to allow for heat dissipation and hence to maintain a constant temperature. The total recording time was 9 h (a) and 12 h (b). The line widths vary between 350 and 600 Hz in spectrum (a) and between 250 and 400 Hz in spectrum (b). The sample contained 700 mg of 5CB. (c) 107.5 MHz ^{2}H–{^{1}H} NMR spectrum of 5CB in the nematic phase at 293 K on a sample contained in a 4 mm rotor and using a 4 mm double resonance CPMAS probe. The spectrum is the result of accumulating 16k free-induction decays into 2988 points, zero filling to 32k and weighting with an exponential window function with a decay rate of 40 Hz before Fourier transformation. SPINAL-64 decoupling was applied on protons during the acquisition of the deuterium spectrum (acquisition time of 14 ms) at a RF field strength of 50 kHz. A 2 s recycle delay was used between pulses in order to avoid sample heating due to high power proton decoupling. The total recording time was about 9 h.

independent of the conformation; (2) the conformational distribution; (3) the values of the quadrupolar tensors, and their orientation in the molecules; (4) the conformationally-dependent order parameters. It is now possible to obtain good estimates for parameters (1) to (3) by calculations with DFT or *ab initio* molecular orbital methods. These calculations were done for 5CB using the software Gaussian (*20*) using the DFT method B3LYP/6-311G**. Table 1 reports the results of calculations of the structure of the

Table 1. The structural parameters of 4-pentyl-4′-cyanobiphenyl in the minimum energy conformation calculated by the DFT B3LYP/6-311G** method. The bond lengths, R_{ij}, are in Å, the bond angles, θ_{ijk}, and the dihehedral angles, δ_{ijkq}, are in degrees.

Atom *i*	Atom *j*	R_{ij}	Atom *k*	θ_{ijk}	Atom *q*	δ_{ijkq}
2	1	1.482				
3	2	1.402	1	121.105		
4	3	1.390	2	120.956	1	180.003
5	4	1.399	3	121.278	2	0.190
6	5	1.399	4	117.722	3	0.033
7	2	1.402	3	117.812	4	−0.166
8	1	1.404	2	121.012	3	38.990
9	8	1.387	1	121.258	2	180.044
10	9	1.402	8	120.054	1	−0.061
11	10	1.402	9	119.350	8	0.027
12	11	1.387	10	120.052	9	0.023
13	10	1.430	9	120.325	8	180.023
14[a]	13	1.156	10	180.0		
15	3	1.0842	2	119.638	1	1.482
16	4	1.0855	3	119.311	2	180.343
17	7	1.0842	2	119.620	1	1.854
18	6	1.0855	7	119.303	2	181.121
19	8	1.0834	9	119.217	10	178.380
20	9	1.0830	8	120.361	1	180.547
21	11	1.0830	12	120.367	1	180.554
22	12	1.0834	11	119.219	10	178.386
23	5	1.511	4	121.147	3	181.584
24	23	1.542	5	113.168	4	90.236
25	24	1.532	23	113.087	5	179.927
26	25	1.533	24	113.512	23	180.147
27	26	1.531	25	113.222	24	179.945
28	23	1.096	5	109.451	24	121.786
29	23	1.096	5	109.451	24	−121.819
30	24	1.096	23	109.055	25	122.292
31	24	1.096	23	109.055	25	−122.262
32	25	1.098	24	109.306	26	122.166
33	25	1.098	24	109.306	26	−122.166
34	26	1.097	25	109.192	27	122.243
35	26	1.097	25	109.192	27	−122.243
36	27	1.093	26	111.423	25	180.022
37	27	1.094	26	111.172	36	120.105
38	27	1.094	26	111.172	36	−120.105

[a]The Gaussian program requires a ''dummy'' atom in order to define a linear fragment such as the C–C≡ N.

minimum energy conformer as elements of a Z matrix, which is the form used by the Gaussian program.

The minimum energy conformer has the two phenyl rings at an angle of 39°, and the alkyl chain is perpendicular to the plane of the attached ring. The alkyl chain is in the extended, all-trans form. Calculations were also done, with full geometry optimization, at the other minimum energy positions obtained by rotation about the bonds C5–C23, C23–C24, C24–C25 and C25–C26. Note that for each rotation the rest of the molecule is maintained rigid. The relative energies of these conformations are given in Table 2.

Table 3 lists the magnitude and orientation of the quadrupolar tensors when the molecule is in the minimum energy structure. These data were calculated from the electric field gradient tensors obtained by the B3LYP/6-311G** calculation using a conversion factor between atomic units and kilohertz of −571.8 kHz/a.u, which was found to provide good agreement between calculated and observed values of the quadrupole tensor components for the mesogenic molecule 4-hexyloxy-4′-cyanobiphenyl (*21*).

The data reported in Table 3 show that the principal components of the quadrupolar tensors at the aromatic sites are very similar, and in each case the largest component is directed along the bond direction to within 0.5°.

The data in Tables 1 and 3 may be used to calculate values of the residual quadrupolar splittings, $\Delta\nu_k(R)$, for the aromatic deuteriums. The rapid motion of the two rings about their para axes leads to

Table 2. Energy differences, ΔE_{ij} (kJ mol^{-1}), calculated by the DFT B3LYP/6-311G** method between the minimum energy conformer and conformers at local energy minima generated by rotation about the C_i–C_j bonds in the alkyl chain of 4-pentyl-4′-cyanobiphenyl. The angle ϕ_{ij} (°) is the position of the secondary minimum.

Bond	ΔE_{ij}	ϕ_{ij}
C_5–C_{23}	5.68	90.4
C_{24}–C_{23}	2.82	66.1
C_{25}–C_{24}	3.75	67.3
C_{26}–C_{25}	3.60	66.3

a simplification of Equation (1) to:

$$\begin{aligned}\Delta\nu_k(R) = \frac{3}{4}q_{aa}(k)[S_{zz}(R)\{(3\cos^2\theta_{azk}-1)\\ +\eta(k)(\cos^2\theta_{bzk}-\cos^2\theta_{czk})\}\\ +(S_{xx}(R)-S_{yy}(R))\{\cos^2\theta_{axk}-\cos^2\theta_{ayk}(4)\\ +\frac{1}{3}\eta(k)\cos^2\theta_{bxk}-\cos^2\theta_{byk}-\cos^2\theta_{cxk}\\ +\cos^2\theta_{cyk}\}]\end{aligned}$$

where the $S_{zz}(R)$ and $S_{xx}(R)-S_{yy}(R)$ are local order parameters for the phenyl rings.

It might be thought possible to guess the values of $S_{zz}(R)$ and $S_{xx}(R)-S_{yy}(R)$ for a mesogen like 5CB with sufficient accuracy to get good approximations to the expected magnitudes of the residual quadrupolar splittings. Thus, it is reasonable to expect $S_{zz}(R) \gg (S_{xx}(R)-S_{yy}(R))$, and hence to set the biaxial order parameter to zero. However, it turns out that this is not a good approximation since the terms in equation (4), which involve $S_{xx}(R)-S_{yy}(R)$, are very important in determining the magnitude of $\Delta\nu_q$ for the aromatic sites. To demonstrate this, the values of the local order parameters were taken from the study (*22*) of the ^{1}H–{^{2}H} spectra of partially-deuterated samples of 5CB. Using $S_{zz}(R)=0.60$ and $S_{xx}(R)-S_{yy}(R)=0.05$ gives the relative order of splittings $\Delta\nu_{15}>\Delta\nu_{16}>\Delta\nu_{19}>\Delta\nu_{20}$, and this is taken to be the same as those observed. The calculated aromatic splittings are compared with those observed in Table 4.

It is important to note the importance of the terms in Equation (5) that involve the biaxial order parameter $S_{xx}(R)-S_{yy}(R)$. These contribute 5.3 kHz to each of the calculated splittings for the aromatic deuteriums. It is also important to note that there is a large sensitivity of the calculations to the geometry of the ring. Thus, because of these two factors it is not possible to use the observed quadrupolar splittings together with the calculated quadrupolar tensors, but fixing the geometry at that calculated by B3LYP/6-311G**, to obtain values for the two order parameters.

Obtaining the conformational distribution for the aliphatic chain from the quadrupolar splittings

Previous studies of the NMR spectra of deuterated samples of 5CB concluded that the relative values of $\Delta\nu_k$ for the aliphatic sites are determined by the averaging effects of rotations about the C–C bonds, and comparing observed quadrupolar splittings with those calculated by various theoretical models is now well-established as a method for obtaining the conformational distribution $P_{LC}(n)$, and for determining the conformationally-dependent order parameters. This subject is revisited here so that it can be compared with the determination of these important properties of a mesogenic molecule from the residual proton–carbon dipolar couplings.

The effect on the residual quadrupolar splittings of averaging over a conformational distribution is given in general by Equation (3), with the values of $\Delta\nu_k(n)$ related to the conformationally-dependent order parameters, $S_{\alpha\beta}(n)$ by Equation (1). It is necessary to adopt a theoretical model for how the order parameters depend on the conformation of the molecule, and this implies choosing a model for how the anisotropic intermolecular forces change as the shape of the molecule changes. This problem is simplified by adopting a mean field approach, that is by introducing a mean potential, $U_{LC}(\beta, \gamma, n)$, for a single molecule in the nth conformation, and at an orientation in the liquid crystalline phase specified by the polar angles β and γ made by the mesophase director in a reference frame fixed in a rigid part of the flexible molecule. This mean potential can always be divided into a totally anisotropic part, $U_{ext}(\beta, \gamma, n)$, and a part, $U_{iso}(n)$, which survives into the isotropic phase, and which can be approximated by the energies of the conformers calculated by the DFT method for an isolated molecule. The order parameters depend only on $U_{ext}(\beta,\gamma,n)$, for example:

$$\begin{aligned}S_{zz}(n) = Z_{ext}^{-1}(n)\int(\frac{3}{2}\cos^2\beta-\frac{1}{2})\\ \exp[-U_{ext}(\beta,\gamma,n)/RT]\sin\beta\,\mathrm{d}\beta\,\mathrm{d}\gamma,\end{aligned} \quad (5)$$

where

$$Z_{ext}(n) = \int\exp[-U_{ext}(\beta,\gamma,n)/RT]\sin\beta\,\mathrm{d}\beta\,\mathrm{d}\gamma. \quad (6)$$

Table 3. The quadrupolar tensors calculated by the DFT B3LYP/6-311G** method for deuterium nuclei in 4-pentyl-4′-cyanobiphenyl when in the minimum energy conformation. The values of $q_{\alpha\alpha}$ were obtained from the electric field gradient tensors by multiplication by −571.8 kHz/a.u. The orientation of each tensor relative to axes *xyz* fixed in the ring containing the deuterium, for aromatic sites, and fixed in the alkylated ring for aliphatic sites, is given as the set of direction cosines, cos $\theta_{\alpha\beta}$, where α is successively *a*, *b* or *c*, which are the principal axes of the quadrupolar tensor, and β is *x*, *y*, or *z*. The asymmetry parameter, η, is also given, as is the direction cosines of the C–D bond, and the angle, θ_{CDa}, between this bond and the direction, *a*, of the largest component of the quadrupolar tensor.

Site		Orientation		
15	q_{aa}	cos θ_{ax}	cos θ_{ay}	cos θ_{az}
	180.7	−0.87236	−0.01989	0.48846
	q_{bb}	cos θ_{bx}	cos θ_{by}	cos θ_{bz}
	−83.7	−0.48733	−0.04406	−0.87211
	q_{cc}	cos θ_{cx}	cos θ_{cy}	cos θ_{cz}
	−96.7	−0.03887	0.99883	−0.02874
η	0.072			
bond direction		0.87230	−0.02247	0.48848
θ_{CDa}	0.5°			
16	q_{aa}	cos θ_{ax}	cos θ_{ay}	cos θ_{az}
	180.2	−0.87038	−0.01270	−0.49221
	q_{bb}	cos θ_{bx}	cos θ_{by}	cos θ_{bz}
	−83.4	−0.47535	0.26846	0.83784
	q_{cc}	cos θ_{cx}	cos θ_{cy}	cos θ_{cz}
	−96.8	0.01038	−0.99991	−0.00873
η	0.074			
bond direction		−0.87070	−0.00417	−0.49181
θ_{CDa}	0.5°			
19	q_{aa}	cos θ_{ax}	cos θ_{ay}	cos θ_{az}
	180.6	−0.86997	0.01866	0.49274
	q_{bb}	cos θ_{bx}	cos θ_{by}	cos θ_{bz}
	−83.7	0.49155	−0.04611	0.86963
	q_{cc}	cos θ_{cx}	cos θ_{cy}	cos θ_{cz}
	−96.9	−0.03895	−0.99876	−0.03095
η	0.073			
bond direction		−0.86934	0.02066	0.49385
θ_{CDa}	0.0°			
20	q_{aa}	cos θ_{ax}	cos θ_{ay}	cos θ_{az}
	180.2	−0.86700	0.00920	−0.49822
	q_{bb}	cos θ_{bx}	cos θ_{by}	cos θ_{bz}
	−83.6	−0.49824	−0.00093	−0.867043
	q_{cc}	cos θ_{cx}	cos θ_{cy}	cos θ_{cz}
	−96.5	0.00844	0.99996	0.00377
η	0.072			
bond direction		−0.86571	0.00939	−0.50054
θ_{CDa}	0.0°			
28	q_{aa}	cos θ_{ax}	cos θ_{ay}	cos θ_{az}
	168.8	−0.79422	−0.50180	0.34265
	q_{bb}	cos θ_{bx}	cos θ_{by}	cos θ_{bz}
	−82.1	−0.56092	0.82229	−0.09593
	q_{cc}	cos θ_{cx}	cos θ_{cy}	cos θ_{cz}
	−86.7	0.23362	0.26839	0.93455
η	0.027			
bond direction		−0.79070	−0.50600	0.34462
θ_{CDa}	0.3°			
30	q_{aa}	cos θ_{ax}	cos θ_{ay}	cos θ_{az}
	168.0	−0.79289	−0.50386	0.34271
	q_{bb}	cos θ_{bx}	cos θ_{by}	cos θ_{bz}
	−81.4	−0.60337	0.57047	−0.55723
	q_{cc}	cos θ_{cx}	cos θ_{cy}	cos θ_{cz}
	−86.6	−0.08526	0.648607	0.75633
η	0.031			
bond direction		−0.78879	−0.50766	0.34649
θ_{CDa}	0.5°			

Table 3. Continued

Site		Orientation		
32	q_{aa}	$\cos\theta_{ax}$	$\cos\theta_{ay}$	$\cos\theta_{az}$
	167.4	−0.79064	0.51074	−0.33767
	q_{bb}	$\cos\theta_{bx}$	$\cos\theta_{by}$	$\cos\theta_{bz}$
	−81.1	0.61228	−0.66025	0.43496
	q_{cc}	$\cos\theta_{cx}$	$\cos\theta_{cy}$	$\cos\theta_{cz}$
	−86.3	0.00079	0.55065	0.83474
η	0.031			
bond direction		−0.78728	0.51392	−0.34077
θ_{CDa}	0.0°			
34	q_{aa}	$\cos\theta_{ax}$	$\cos\theta_{ay}$	$\cos\theta_{az}$
	168.6	−0.79033	−0.51031	0.33906
	q_{bb}	$\cos\theta_{bx}$	$\cos\theta_{by}$	$\cos\theta_{bz}$
	−82.1	−0.61201	0.63161	−0.47592
	q_{cc}	$\cos\theta_{cx}$	$\cos\theta_{cy}$	$\cos\theta_{cz}$
	−86.5	−0.02871	0.58365	0.81150
η	0.026			
bond direction		−0.78766	−0.51362	0.34031
θ_{CDa}	0.0°			
36	q_{aa}	$\cos\theta_{ax}$	$\cos\theta_{ay}$	$\cos\theta_{az}$
	173.9	−0.02314	0.93799	0.34587
	q_{bb}	$\cos\theta_{bx}$	$\cos\theta_{by}$	$\cos\theta_{bz}$
	−85.1	0.9997	0.02400	0.00178
	q_{cc}	$\cos\theta_{cx}$	$\cos\theta_{cy}$	$\cos\theta_{cz}$
	−88.7	0.00662	−0.34582	0.93828
η	0.021			
bond direction		−0.02311	0.93675	0.34922
θ_{CDa}	0.3°			
37	q_{aa}	$\cos\theta_{ax}$	$\cos\theta_{ay}$	$\cos\theta_{az}$
	172.5	−0.79791	−0.48088	0.36343
	q_{bb}	$\cos\theta_{bx}$	$\cos\theta_{by}$	$\cos\theta_{bz}$
	−84.2	−0.53739	0.84063	−0.06754
	q_{cc}	$\cos\theta_{cx}$	$\cos\theta_{cy}$	$\cos\theta_{cz}$
	−88.3	0.27303	0.24919	0.92917
η	0.024			
bond direction		−0.79621	−0.48063	0.36575
θ_{CDa}	0.2°			

Attention now focuses on $U_{ext}(\beta, \gamma, n)$, and here we adopt the additive potential (AP) model (*23*). This starts by expressing $U_{ext}(\beta, \gamma, n)$ in the general form:

$$U_{ext}(\beta, \gamma, n) = -\varepsilon_{2,0}(n)C_{2,0}(\beta) - 2\,\mathrm{Re}\,\varepsilon_{2,2}(n)C_{2,2}(\beta, \gamma), \quad (7)$$

where the $C_{2,m}(\beta,\gamma)$ are modified spherical harmonics (*24*), and the $\varepsilon_{2,m}(n)$ are conformation-dependent interaction parameters. Equation (7) contains too many unknown parameters to be useful, and the important step in the AP method is to relate the $\varepsilon_{2,m}(n)$ to a set of conformation-independent interaction parameters, $\varepsilon_{2,m}(j)$, for each rigid sub-unit in the molecule:

$$\varepsilon_{2,m}(n) = \sum_q \sum_p \varepsilon_{2,p}(j) D^2_{p,m}(\Omega_{jn}). \quad (8)$$

The Wigner functions, $D^2_{p,m}(\Omega_{jn})$ describe the orientation of fragment j to reference axes in the nth

Table 4. The residual quadrupolar splittings, $\Delta\nu_k$ (kHz), measured from the ^{2}H spectrum of the deuterium atoms at natural abundance in a sample of 4-pentyl-4′-cyanobiphenyl at 107.5 mHz and 293 K. The calculated values for the aromatic sites are those obtained using the calculated geometry and quadrupolar tensors given in Tables 2 and 3, and assuming values of local order parameters of $S_{zz}(R)=0.60$, $S_{xx}(R)-S_{yy}(R)=0.05$. The calculated values for the aliphatic sites were obtained by averaging over all the conformations whose relative populations were those calculated from the energy differences in Table 2.

	$\Delta\nu_k$/kHz	
Site, k	Observed	Calculated
15	−14.783 ± 0.020	−13.22
16	−14.221 ± 0.020	−12.63
19	−13.644 ± 0.020	−12.26
20	−11.175 ± 0.020	−11.04
28	−58.433 ± 0.020	−58.301
30	−41.647 ± 0.020	−41.605
32	−44.262 ± 0.020	−44.360
34	−30.687 ± 0.020	−30.237
36	−22.174 ± 0.020	−22.164

conformation. For 5CB the fragment tensors are chosen to be:

$\varepsilon_{zz}(R)$, directed along the z axis of the biphenyl group;

$\varepsilon_{3,7} = \varepsilon_{8,12}$

$\varepsilon_{5,24}$

$\varepsilon_{23,25} = \varepsilon_{24,26} = \varepsilon_{25,27}$

$\varepsilon_{30,31} = \varepsilon_{32,33} = \varepsilon_{34,35}$.

The geometry, the conformation parameters, ΔE_{tg}, and the values of the quadrupolar tensors, $q_{CD}(k)$, are taken from the results of the DFT calculations. Here $q_{CD}(k)$ is the component along the C–D bond at site k in the aliphatic chain, and equated with the calculated value of $q_{aa}(k)$, and the asymmetry parameters are set to zero. The calculated values of $\Delta\nu_q$ for the five positions in the aliphatic chain are brought into best agreement with those observed by varying the four interaction parameters $\varepsilon_{zz}(R)$, $\varepsilon_{5,24}$, $\varepsilon_{23,25}=\varepsilon_{24,26}=\varepsilon_{25,27}$, and $\varepsilon_{30,31}=\varepsilon_{32,33}=\varepsilon_{34,35}$.

The agreement between calculated and observed values of $\Delta\nu_k$ is very good, as shown in Table 4. The main interest here in these calculations is that they allow good estimates to be made of the ^{13}C–^{1}H residual dipolar couplings, and hence to assign the splittings in the PDLF spectrum. It is interesting to note, however, that the close agreement between observed and calculated residual quadrupolar splittings for the chain positions was achieved with the bond lengths and angles, and the energy differences ΔE_{ij} calculated by the B3LYP/6-311G** method. Previous applications of the AP method to calculating the chain quadrupolar splittings used a different parameterisation for the interaction tensors $\varepsilon_{2,m}(j)$, and assumed that ΔE_{ij} is the same for all three bonds (*19*), and a value of $\Delta E_{ij}=3.27\pm0.01\,\mathrm{kJ\,mol^{-1}}$ was obtained, which compares well with the three separate values of 2.82, 3.75 and $3.60\,\mathrm{kJ\,mol^{-1}}$ used in the present calculation. Note that a better fit to the data is obtained with the three, fixed values of ΔE_{ij} than with a single, optimised value.

4. The ^{13}C, ^{1}H PDLF experiments

A larger data set is obtained from the PDLF experiment than from the deuterium natural abundance spectrum, and the problem of assignment is correspondingly more challenging. The aim of the PDLF experiment is to obtain the residual dipolar couplings between each ^{13}C nucleus in the molecules, at natural abundance, and the protons. A simple, single pulse ^{13}C spectrum of a molecule as large as 5CB is too complex for analysis, and does not yield values of any of the dipolar couplings. The main reason for the complexity is that all the protons are strongly coupled to each other, and this directly affects the spectrum from each ^{13}C nucleus. The total spectrum is therefore an overlapping set of intractable second-order sub-spectra. The key aspects of the PDLF experiment is to separate the spectra from each ^{13}C nucleus by using a two-dimensional experiment and to remove the effects of the strong proton–proton dipolar coupling by decoupling the protons from each other in the t_1 dimension (see Figure 1). The methods used for this homonuclear dipolar decoupling lead to a scaling of the total spin–spin residual couplings to the ^{13}C nuclei so that the splittings observed on each ^{13}C resonance are given by

$$\Delta_{ij} = k\left(J_{ij} + 2D_{ij}\right) \tag{9}$$

Calibration of the PDLF experiment

It is possible to obtain a value for k by recording a 1D ^{13}C spectrum of a solute dissolved in a liquid crystalline solvent with and without application of the homonuclear decoupling sequence to the protons. The solute is chosen such that it has a readily analyzable ^{13}C spectrum. Fung *et al.* (*25*) used this method, with benzene as the solute, to calibrate the sequences MREV-8, BLEW-48, FSLG-2 and MDHOT-3. However, this method has a disadvantage which stems from the temperature sensitivity of the residual dipolar couplings. Application of the homodecoupling sequence may raise the temperature of the sample and there is no way of detecting that such a change has occurred. The approach adopted here is to use fluorobenzene as the solute, and also to compare the results from 1D ^{1}H and ^{19}F, including detection of ^{13}C satellite lines, to those from a PDLF 2D experiment. In this case the PDLF spectrum depends on unscaled residual ^{13}C–^{19}F couplings so that these can be used to detect whether there is a change in orientational order of the solute between experiments, and to apply a correction if necessary. Figure 4 shows the spectra obtained for the sample of fluorobenzene (Aldrich) approximately 10 wt% dissolved in the nematic solvent ZLI 1695 (Merck, Darmstadt), which was chosen because it does not contain aromatic groups.

The spectra from the all-^{12}C molecules (the strong lines) were analysed first using a graphical interactive procedure dubbed ARCANA (*26*) to give the spectral

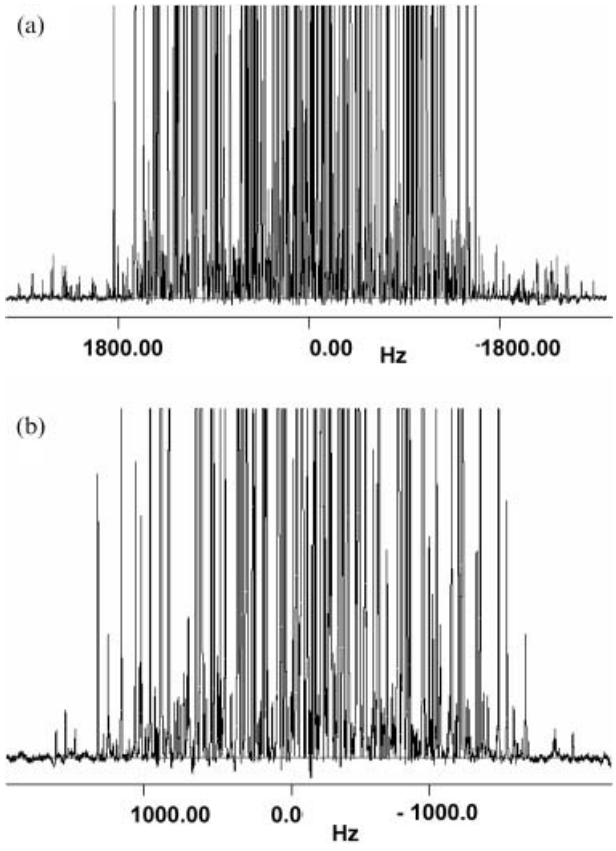

Figure 4. (a) 500 MHz ^{1}H and (b) 470 MHz ^{19}F spectra of fluorobenzene approximately 10 wt% in the nematic solvent ZLI 1695 at 300 K. Each spectrum is the result of Fourier transforming the average of 2k free-induction decays accumulated into 64k of computer memory. Note that some of the strongest lines are truncated in order to reveal the weak lines from the molecules containing a single ^{13}C nucleus.

parameters of Table 5. The scalar couplings, J_{ij}, in Table 5 were kept fixed at the values reported in the literature (*27, 28*). The values obtained for D_{HH}, D_{HF} and chemical shifts were then kept constant in the analysis of satellite spectra. Trial values of D_{CH} and D_{CF} for each isotopomer were calculated using as order parameters the values calculated from the D_{HH} and D_{HF} coupling. To facilitate the analysis of satellite spectra the program ARCANA has been modified to display calculated spectra including transitions from all the isotopomer spin systems, with properly scaled intensities. The final dipolar couplings obtained are given in Table 5.

This same sample was then used to obtain a ^{13}C–{^{1}H} (Figure 5), and a PDLF spectrum (Figure 6) in each case on the 700 MHz spectrometer.

The residual couplings D_{CF} for carbons C2–C4 appear in both the spectra of Figure 5 and Figure 6, and are compared in Table 5. They are essentially unchanged in value, which confirms that the two spectra were recorded with the same orientational order of the fluorobenzene molecules.

The sections at the chemical shifts of the ^{13}C in the F_1 domain of the 2D PDLF ^{13}C spectrum yield scaled splittings, $k\Delta_{ij}$(PDLF) between the carbon and the protons, which are given in Table 5. Comparing these with the total spin–spin couplings Δ_{ij}(500) allows values of the scaling factor k to be derived, and an average value of 0.47 ± 0.02 to be obtained.

5. The ^{13}C–{^{1}H } spectrum of 5CB

A ^{13}C–{^{1}H} spectrum of 5CB was recorded at 176 MHz, and is shown in Figure 7.

The most important point for obtaining good spectra on liquid crystalline samples is to prevent the temperature rising during acquisition since this will lead to a broadening of the lines. The efficiency of the proton decoupling must be combined with a delay between acquisitions to allow for heat dissipation, and here the decoupling was achieved with the composite pulse method SPINAL-64, and a delay between pulses of 10 s.

The assignment of this spectrum has been published previously, but here we are concerned to use 5CB as a general example, and to discuss the general approaches that can be used for assigning the peaks. The ^{13}C–{^{1}H} spectrum of an isotropic sample can usually be assigned by a combination of 2D experiments, particularly HSQC and INADEQUATE and the assignment for 5CB has been done previously by these methods (*29*). These methods are not applicable to liquid crystalline samples because of the strong, second-order effects on the proton spectrum, and the large range of values of the ^{13}C–^{1}H total spin–spin couplings. The chemical shifts of the ^{13}C nuclei in the liquid crystalline phase have a contribution from the anisotropy in the chemical shift tensor, which means that they may differ considerably from those in the isotropic phase. It is possible to distinguish aliphatic from aromatic carbons in the liquid crystalline phase but their relative positions may have changed from the isotropic phase.

It is possible to correlate the ^{13}C chemical shifts with the deuterium residual quadrupolar splittings in deuterium-enriched compounds, and this method has been applied to a sample of fully deuterated 5CB (*30, 31*).

6. The ^{13}C, ^{1}H 2D PDLF spectrum of 5CB

Figure 8 shows the 2D PDLF spectrum recorded on 5CB at 293 K.

Table 5. NMR parameters D_{ij}(500) (Hz) obtained from the analysis of the ^{1}H and ^{19}F spectra at 11.74 T and 300 K; D_{ij}(700) (Hz) from the ^{13}C–{^{1}H}spectrum of the sample in the MAS rotor, and $k\Delta_{ij}$(PDLF)/Hz obtained from the 176 MHz PDLF ^{13}C spectrum of a sample of fluorobenzene dissolved in the nematic solvent ZLI 1695 at 293 K.

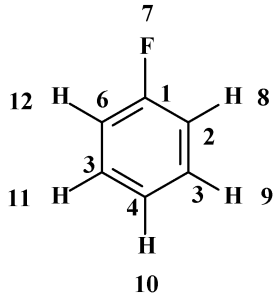

i,*j*	J_{ij}	D_{ij}(500)	Δ_{ij}(500)	D_{ij}(700) 1D spectrum	D_{ij}(700) 2D spectrum	$k\Delta_{ij}$(PDLF)
1,7	−245.80	704.78 ± 0.14				
1,8	−4.89	139.30 ± 0.12				
1,9	10.95	47.26 ± 0.13				
1,10	−1.73	36.01 ± 0.16				
2,7	20.80	121.28 ± 0.11		122 ± 1	122 ± 1	
2,8	162.55	1156.97 ± 0.12	2476.49			1173 ± 6
2,9	1.10	188.63 ± 0.15	378.36			169 ± 1
2,10	8.29	49.63 ± 0.14				
2,11	−1.50	26.37 ± 0.16				
2,12	4.11	35.84 ± 0.13				
3,7	7.91	35.69 ± 0.18		36 ± 1	37 ± 1	
3,8	−0.57	181.21 ± 0.16				164 ± 1
3,9	161.14	1145.80 ± 0.17	2452.74			1169 ± 5
3,10	9.02	176.40 ± 0.19	361.82			164 ± 1
3,11	1.74	33.61 ± 0.21				
3,12	0.76	30.61 ± 0.20				
4,7	3.18	27.65 ± 0.11		23 ± 1	23 ± 1	
4,8	7.57	45.18 ± 0.16				
4,9	0.82	138.69 ± 0.15	278.20			142 ± 0.5
4,10	161.37	1477.48 ± 0.18	3116.33			1449 ± 10
7,8	9.31	344.28 ± 0.08				
7,9	5.79	77.17 ± 0.09				
7,10	0.34	53.56 ± 0.09				
8,9	8.00	504.51 ± 0.08				
8,10	2.00	91.51 ± 0.08				
8,11	0.00	50.68 ± 0.08				
8,12	2.00	71.90 ± 0.13				
9,10	7.90	398.96 ± 0.07				
9,11	2.00	70.44 ± 0.13				

The splittings, Δ_{ij}, obtained are given in Table 6. To determine the values of D_{ij} from Equation (7) it is necessary to know the values of the scalar couplings, J_{ij}. In principle it is possible to obtain the magnitudes and signs of the large, one-bond couplings from variable angle spinning experiments (*32–34*), but this method was not available to us. Alternatively the couplings can be obtained from spectra of the sample dissolved in $CDCl_3$. The values of $^{1}J_{CH}$ are easily obtained from the ^{13}C spectrum of this sample or to simplify the multiplet using ^{13}C J-resolved Bird experiments (*35*). The smaller splittings on each ^{13}C peak are more difficult to assign, and their magnitudes, but not their signs, were obtained by using HetSERF experiments (*36*). This pulse sequence is a heteronuclear J-resolve experiment where the 180° proton pulse is a selective pulse, so that in the 2D experiments, the t_1 signal is modulated only by the couplings between the each of the carbons and the selected proton. The experiment was repeated for each of the resolved proton resonances. The results are shown in Table 6.

The possibility of determining the signs of $^{2}J_{CH}$ and $^{3}J_{CH}$ by calculating their values has been explored. The calculations were done using the gauge-invariant atomic orbitals method (GIAO) with the program G03. The results obtained by this method are dependent on the wavefunctions used

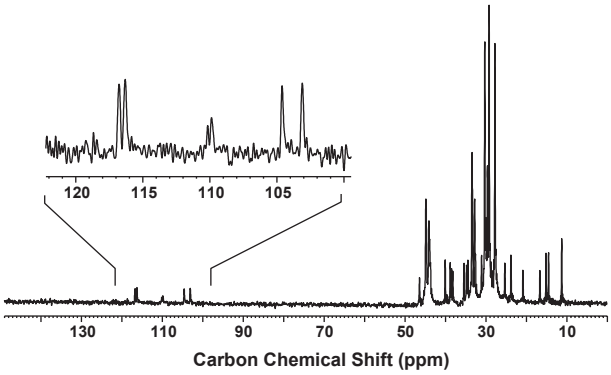

Figure 5. Single pulse 176 MHz ^{13}C–$\{^1H\}$ spectrum on a sample of fluorobenzene dissolved in the Merck nematic liquid crystalline solvent ZLI 1695 at 293 K. The number of scans was 64 with a recycle delay of 6 s. During acquisition of the carbon signal (acquisition time of 30 ms), SPINAL-64 (*13*) decoupling was applied at a RF field of 50 kHz. Note that the resonance of the carbon-13 nucleus directly attached to the fluorine is not visible in this spectrum.

(*37*), and here the density functional approach was adopted to calculate the wavefunctions appropriate for a fully geometrically-optimised structure with the density functional B3LYP and with the Gaussian basis sets 6-31G* and 6-311G**. The calculated values are shown in Table 6, where it is seen that the values obtained are basis set dependent, and those obtained with the 6-311G** basis set gives results for $^1J_{CH}$ and $^3J_{CH}$ that are closer to those observed, and sufficient to unambiguously determine the signs for all the measured values. This is not the case however for the values of $^2J_{CH}$. For the couplings involving an aromatic proton the calculated values are all close to zero, whereas those observed have a magnitude close to 4 Hz. For couplings involving an aliphatic proton the calculated values of $^2J_{CH}$ are all negative and close to −4 Hz. On this evidence the values of $^2J_{CH}$ involving an aliphatic proton were assigned a negative sign, whereas those involving an aromatic proton were regarded as indeterminate in sign, and were therefore set to a zero value when determining the values of the residual dipolar couplings using Equation (9).

The assignment of the splittings to the particular ^{13}C and ^1H nuclei was achieved in the following stages.

The aliphatic carbons

The assignment of the chemical shifts of the aliphatic carbons can be achieved by noting that the one-bond residual dipolar couplings, ^1D_k, for the carbon at site k are approximately proportional to the quadrupolar splittings $\Delta\nu_k$. Thus,

$$^1D_k = -K_{CH} r_{CHk}^{-3} S_{CHk}, \qquad (10)$$

where

$$K_{CH} = \mu_0 \gamma_C \gamma_H h / (16\pi^3) \qquad (11)$$

and S_{CHk} is the orientational order parameter for the C–H bond which has a length of r_{CHk}. If the effect on $\Delta\nu_k$ of the asymmetry parameter [see Equation (1)]

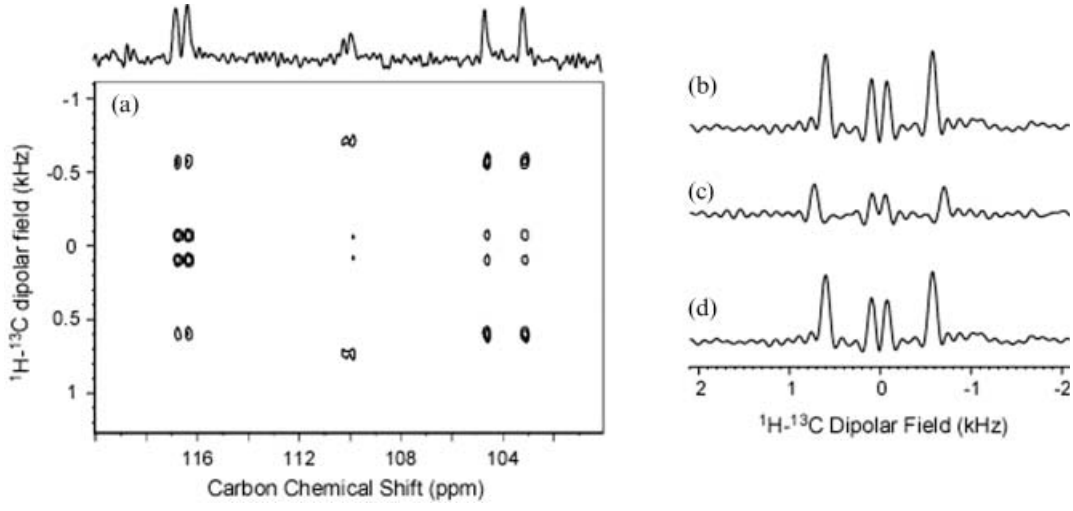

Figure 6. (a) Extract in the aromatic region from a two-dimensional PDLF spectrum of fluorobenzene dissolved in the Merck nematic liquid crystalline solvent ZLI 1695 at 293 K. A total of 128 t_1 increments with 80 scans each were acquired with a recycle delay of 6 s. The total acquisition time was 17 h. Other experimental details are given in the experimental section. (a), (b) and (c) shows F_1 traces extracted respectively at 116.7, 110.1 and 104.6 ppm (right-handed resonance of each doublet). Note that the resonance of the carbon-13 nucleus directly attached to the fluorine is not visible in this spectrum.

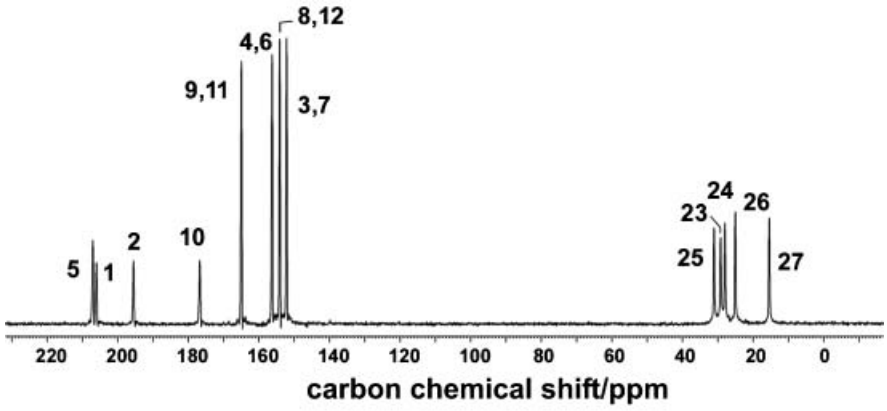

Figure 7. One-dimensional 176 MHz ^{13}C spectrum of 4-pentyl-4′-cyanobiphenyl at 293 K. the spectrum was obtained after cross-polarization from protons (CP contact time of 1.5 ms). The number of scans was 16 and the recycle delay 10 s. During acquisition of the carbon signal (acquisition time of 30 ms), SPINAL-64 (*13*) decoupling was applied at a RF field of 50 kHz.

can be neglected, and if the largest principal component, $q_{aa}(k)$ of the quadrupolar tensor can be assumed to lie along the C–D bond, which the data in Table 3 shows is reasonable for the aliphatic sites, then

$$\Delta\nu_k = \frac{3}{2} q_{\mathrm{CD}k} S_{\mathrm{CD}k}, \tag{12}$$

where $S_{\mathrm{CD}k}$ is the order parameter for the C–D bond and this can be equated to $S_{\mathrm{CH}k}$. Thus, the ratio $R_{\mathrm{CH}k}$ of the quadrupolar splitting to the residual dipolar coupling is given approximately by

$$R_{\mathrm{CH}k} = -3 q_{\mathrm{CD}k} r_{\mathrm{CH}k}^3 / 2K_{\mathrm{CH}}. \tag{13}$$

The value of $R_{\mathrm{CH}k}$ can be estimated to be approximately 11–12, and this allows the relative values of $^1D_{\mathrm{CH}k}$ to be obtained. The splittings $^1\Delta_{\mathrm{CH}k}$ can then be estimated using Equation (9) and the measured values of $^1J_{\mathrm{CH}k}$, and hence an assignment of the aliphatic chemical shifts can be made.

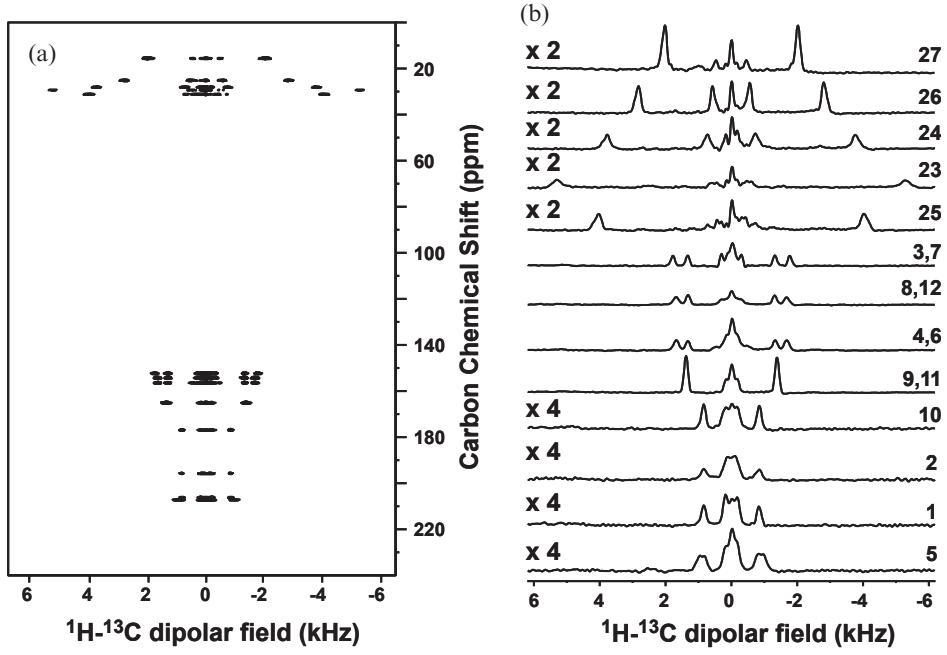

Figure 8. (a) Two-dimensional 176 MHz ^{1}H-^{13}C PDLF spectrum of 5CB recorded at 293 K. A total of 256 t_1 increments with eight scans each were collected with a recycle delay of 10 s (total experimental time of 5 h and 40 min). The total acquisition times were 15 ms in both dimensions. The scale in the dipolar field dimension has been corrected by the scaling factor determined experimentally on the fluorobenzene sample (k=0.47). (b) F_1 traces extracted for the various carbon-13 resonances of 5CB.

Table 6. The splittings, Δ_{ij} (Hz), obtained from the 176 MHz PDLF ^{13}C spectrum of a sample of 5CB at 293 K, and the residual dipolar couplings, D_{ij}, derived from the splittings using the values of J_{ij} (Hz) and the scaling factor of 0.47. The values of the scalar coupling constants, J_{ij}(calc), calculated with the B3LYP/6-31G* and B3LYP/6-311G** wavefunctions are also given.

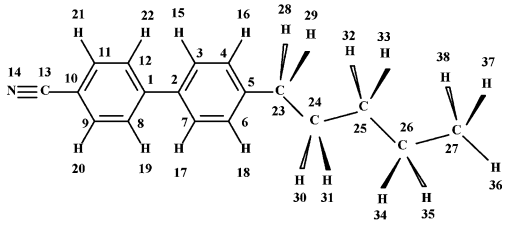

				J_{ij}(calc)	
i,*j*	Δ_{ij}[a]	J_{ij} (expt)	D_{ij}[b]	31G*	311G**
1,19	783		833	−0.28	0.4
1,20	−172		−183	6.09	6.7
2,15	789		839	−0.3	0.4
2,16	−172	7.8	−187	6.1	6.7
3,15	1655	156.9	1682	136.5	147.7
3,16	−1237	±4.2	−1316[c]	0.0	1.5
3,17		6.7		5.2	5.8
3,19	−279		−297	−0.1	0.03
4,15	−1240	±4.0	−1319[c]	−0.6	0.8
4,16	1568	156.7	1590	136.5	147.1
4,18	153	+7.2	159	5.4	6.0
4,28	−434	+5.2	−464	5.4	5.8
5,15	−186	+7.3	−201	5.9	6.5
5,16	800		851	0.07	0.8
5,28	−956	−5.8	−1014	−3.5	−4.6
5,30		3.5			1.9
8,15	271		288	−0.1	0.05
8,19	1568	161.9	1587	140.0	151.1
8,20	−1231		−1309	−0.3	1.2
8,22	177		188	5.1	5.7
9,19	−1296		−1379	0.03	1.5
9,20	1296	165.5	1296	142.1	154.3
9,21	167	+7	174	5.0	5.7
10,20	788	±4.6	838[c]	−0.5	0.3
10,19	−170	+9.1	−185	0.03	7.8
15,23	−145		−154[c]	0.3	0.3
23,28	4948	126.2	5201	136.0	122.2
23,30	563	−4.4	601	−1.3	−3.2
23,32	−426		−453	2.0[d]	2.3
24,28	682	−5.1	728	−2.4	−4.1
24,30	3517	125.5	3679	133.7	122.6
24,32	−682		−726[c]	−1.5	−3.4
24, 34	−158		−168[c]	1.9[d]	2.2
25,30	−677	−4.2	−718	−1.3	−3.2
25,32	3763	124.6	3941	131.0	119.9
25,34	404	−4.2	432	−1.4	−3.3
25, 36	−290		−308[c]		
26,30	−531	3.5	−567	1.9	2.2
26,32	531	−4.3	567	−1.6	−3.4
26,34	2627	124.4	2732	131.1	121.0
26,36	−531	−4.3	−567	−1.4	−2.4
27,32	−157		−167[c]	2.1	2.3
27,34	−429		−456[c]	−1.7	−3.2
27,36	1887	124.4	1945	125.7	121.3
27,38	1887	124.4		126.3	120.6
27,39	1887	124.4		126.3	120.6

[a]The errors on measuring Δ_{ij} are ±5 Hz. [b]The errors on the values of D_{ij} are ±6 Hz. [c]Value obtained with J_{ij}=0. [d]For the ttt conformer.

The values of $^1D_{ij}$ are averages over the conformational motion, and for a discrete set are given by [cf. Equation (3)]:

$$D_{ij} = \sum_n D_{ij}(n) P_{LC}(n), \tag{14}$$

where $D_{ij}(n)$ is the dipolar coupling between nuclei i and j when the molecule is in the nth rigid conformation, and is given by

$$\begin{aligned} D_{ij}(n) = -K_{ij}(n)\big[&S_{zz}(n)\left(3\cos^2\theta_{ijz}-1\right) \\ &+\left(S_{xx}(n)-S_{yy}(n)\right)\left(\cos^2\theta_{ijx}-\cos^2\theta_{ijy}\right) \\ &+4S_{xy}(n)\cos\theta_{ijx}\cos\theta_{ijy} \\ &+4S_{xz}(n)\cos\theta_{ijx}\cos\theta_{ijz}+4S_{yz}(n)\cos\theta_{ijy}\cos\theta_{ijz}\big] \end{aligned} \tag{15}$$

with

$$K_{ij}(n) = \mu_0\gamma_i\gamma_j h \Big/ 16\pi^3 r_{ijn}^3. \tag{16}$$

The AP method, as applied above with quadrupolar splittings as the data set, is now used to compare calculated and observed values of $^1D_{\mathrm{CH}k}$ to obtain the parameters in Equations (12) and (13), which are then used to predict values for all other residual dipolar couplings. This allows assignments shown in Table 6 to be made for the splittings Δ_{ij} involving the aliphatic carbons.

The aromatic carbons

The splittings involving ^{13}C and ^{1}H nuclei in the aromatic fragment are more difficult to assign. The AP calculations described above do not give a good estimate for the small biaxial ordering $S_{xx}(R)-S_{yy}(R)$ in the local order matrix for the biphenyl group, and this leads to poor estimates for the values for the residual couplings in this group. However, good estimates can be obtained for the residual couplings between nuclei in each of the two rings using values of $S_{zz}(R)=0.56$ and $S_{xx}(R)-S_{yy}(R)=0.05$, as described also for the quadrupolar splittings. This leads to the assignment of the splittings given in Table 6.

Refining the ring structure.

The residual couplings between nuclei within each ring can now be used to obtain values for the angles θ_{HCC}. The variables are $S_{zz}(R)$, $S_{xx}(R)-S_{yy}(R)$ and the angles $\theta_{15,3,4}$, $\theta_{16,4,3}$, $\theta_{19,8,9}$, $\theta_{20,9,8}$. These were varied to produce the best least squares fit to 18 residual dipolar couplings. The results are shown in Table 7.

Rotation about the inter-ring bond

The PDLF experiment yielded the value of just one residual dipolar couplings, $D_{3,19}=D_{3,22}=D_{7,19}=D_{7,22}$, which depends on the averaging produced by rotation about the inter-ring C–C bond. However, this single coupling can be used to explore the form of $P_{LC}(\phi_R)$, the probability that the inter-ring torsion angle has a value between ϕ_R and ϕ_R+dϕ_R. To do this it is necessary to use Equations (14) and (15), with ϕ_R replacing n, together with the AP method to calculate conformationally-dependent, local order parameters, $S_{\alpha\beta}(R)$. There are two rigid fragments, the two phenyl rings, which each contributes $\varepsilon_{zz}(R)$ and $\varepsilon_{3,7}(R)=\varepsilon_{8,12}(R)$. The label R means that these fragment interaction tensor components are for use only for calculating the ring order parameters, and not order parameters for the whole molecule. In the AP method the conformational probability $P_{LC}(n)$ depends upon both inter and intramolecular interactions. Thus, writing the mean potential energy of a molecule in the liquid crystalline phase as

$$U_{LC}(\beta, \gamma, \phi_R) = U_{ext}(\beta, \gamma, \phi_R) + U_{\mathrm{int}}(\phi_R), \tag{17}$$

where $U_{int}(\phi_R)$ is the potential energy for rotation through the angle ϕ_R. Two probability distribution

Table 7. The bond angles, $\theta_{i,j,k}$, and local order parameters, $S_{zz}(R)$, $S_{xx}(R)-S_{yy}(R)$, for the two phenyl groups obtained by fitting calculated residual dipolar couplings, D_{ij}(calc), to those observed, D_{ij}, between ^{13}C and ^{1}H nuclei within each ring in 5CB.

i,j	D_{ij}(calc)/Hz	D_{ij}/Hz	$[D_{ij}(\mathrm{calc})-D_{ij}]$/Hz
1,19	842	838	4
1,20	−196	−193	3
2,15	834	839	−5
2,16	−194	−187	7
3,15	1682	1682	0
3,16	−1330	−1316	−14
4,15	−1326	−1319	7
4,16	1589	1590	−1
5,15	−193	−201	8
5,16	840	851	11
8,19	1588	1587	1
8,20	−1319	−1309	−10
9,19	−1346	−1379	33
9,20	1296	1296	0
9,21	200	174	26
10,19	−194	−185	−9
10,20	848	838	10
i,j,k	θ/°		
15,3,4	119.61 ± 0.07		
16,4,3	119.45 ± 0.07		
19,8,9	119.31 ± 0.07		
20,9,8	120.77 ± 0.07		
$S_{zz}(R)$	0.606 ± 0.002		
$S_{xx}(R)-S_{yy}(R)$	0.039 ± 0.003		

functions can be defined:

$$P_{LC}(\phi_R) = Q_{LC}^{-1} \int \exp[-U_{LC}(\beta, \gamma, \phi_R)/k_BT]\sin\beta\,\mathrm{d}\beta\,\mathrm{d}\gamma \quad (18)$$

with

$$Q_{LC} = \int \exp[-U_{LC}(\beta, \gamma, \phi_R)/k_BT]\sin\beta\,\mathrm{d}\beta\,\mathrm{d}\gamma\,\mathrm{d}\phi_R \quad (19)$$

and

$$P_{iso}(\phi_R) = Q_{iso}^{-1}\exp[-U_{\mathrm{int}}(\phi_R)/k_BT] \quad (20)$$

with

$$Q_{iso} = \int \exp[-U_{\mathrm{int}}(\phi_R)/k_BT]\mathrm{d}\phi_R. \quad (21)$$

The usual way of applying the AP method for investigation of a rotation about a bond has been to use Equations (18)–(21) with a specific form for the bond-rotation potential $U_{int}(\phi_R)$, such as a cosine expansion:

$$U_{\mathrm{int}}(\phi_R) = V_2\cos 2\phi_R + V_4\cos 4\phi_R. \quad (22)$$

The position of the minimum in this function is at

$$\phi_{\min} = \frac{1}{2}\left[\cos^{-1}(-V_2/4V_4)\right]. \quad (23)$$

This function could be used in the present case, but only by fixing one of the coefficients since there is only one residual dipolar coupling which is sensitive to the form of $U_{int}(\phi_R)$. The form of Equation (22), however, is unnecessarily restrictive on the form of both $P_{iso}(\phi_R)$ and $P_{LC}(\phi_R)$, and an alternative method has been suggested (*38*) which uses a sum of Gaussian functions to model $P_{iso}(\phi_R)$ directly. Thus,

$$P_{iso}(\phi_R) = \left[8\pi h^2\right]^{-\frac{1}{2}}\left[\exp\left(-\{\phi_R-\phi_{\min}\}^2\Big/2h^2\right) + \exp\left(-\{\phi_R-180-\phi_{\min}\}^2\Big/2h^2\right)\right]. \quad (24)$$

This function contains two unknowns, ϕ_{min}, which is to be obtained by comparing calculated with observed residual dipolar couplings, and h, the width at half maximum height, and which in the present case has to be fixed.

It is also necessary to eliminate conformations which are strongly hindered by a close approach of atoms. This is achieved by multiplying $P_{iso}(\phi_R)$ by $P_{steric}(\phi_R)$:

$$P_{steric}(\phi_R) = \exp[-U_{steric}(\phi_R)/RT], \quad (25)$$

with

$$U_{steric}(\phi_R) = \sum_{i<j} A_{ij}\Big/r_{ij\phi_R}^{12}. \quad (26)$$

The summation is over just the hydrogen atoms at positions 15, 17, 19 and 22, and a value for A_{ij} was chosen of 1.1 J Å^{12} (*39*), which is sufficient to eliminate severely hindered conformations.

To apply the AP method to the averaging over rotation about the inter-ring bond in the biphenyl fragment the interaction parameters chosen were: $\varepsilon_{zz,}(R)$, which acts along the C1–C2 bond, and $\varepsilon_{3,7}(R)=\varepsilon_{8,12}(R)$, which act along C3–C7 and C8–C12. Note that these interaction parameters are fixed by the values of the residual couplings between C and H nuclei within each phenyl ring. Calculations were done with fixed values of h in the range 10 to 20 Hz, and this gave values for ϕ_{min} in the range 34° to 32°, which is in good agreement with the value of $38.4\pm0.1^\circ$ obtained (*40*) by an AP analysis of the full set of H–H residual dipolar couplings measured by Sinton *et al.* (*41*). Note that the analysis by Celebre *et al.* (*40*) used the cosine expansion for $U_{int}(\phi_R)$, and an allowance was not made for steric interactions; both factors could contribute to the different values obtained for ϕ_{min}. Note also that neither analysis has taken into account the effect on the residual couplings of small-amplitude vibrational motion (*42–44*). The evidence from smaller molecules is that vibrational averaging can change residual dipolar couplings by as much as ~10%, and the effect varies with the type of nuclei involved, and their geometrical disposition. In principle, it is possible to calculate the corrections to residual dipolar couplings using vibrational force fields calculated by either *ab initio* or DFT methods (*45, 46*), but a reliable procedure for flexible molecules as large as 5CB has yet to be developed.

For this inter-ring rotation the probability distributions $P_{iso}(\phi_R)$ and $P_{LC}(\phi_R)$ are practically identical for 5CB in the nematic phase.

The value obtained for $\phi_{\min}$ by the NMR experiments is close to that of 39.0° calculated by the B3LYP/6-311G** method, and given in Table 1, but considerably different from the value of $26.3\pm0.3^\circ$ obtained by X-ray crystallography for crystalline 5CB (*47*).

Rotation about the ring-chain bond

Three residual dipolar couplings, $D_{23,29}=D_{23,30}$, $D_{4,29}=D_{4,30}=D_{6,29}=D_{6,30}$ and $D_{5,29}=D_{5,30}$, are

resolved that depend on the averaging over the rotation about the C5–C23 bond. This bond rotation was investigated in a similar way to that used for the rotation about the inter-ring bond, i.e. by using the Gaussian probability approach [Equations (24)–(26)]. There are therefore two parameters, $h_{23,24}$ and ϕ_{min}(C23–C24) which describe $P_{iso}(\phi_{23,24})$. The symmetry of the phenyl-CH_2 fragment means that three fragment interaction parameters have to be used, and these were chosen to be ε_{zz}(RCH), $\varepsilon_{3,7}$(RCH) and $\varepsilon_{23,24}$(RCH), which is directed along the C23–C24 bond. The label RCH denotes that these parameters have values appropriate for the biphenyl-CH_2 group only. These five parameters were adjusted to give best, least-squares agreement between seven calculated and observed residual dipolar couplings. When the geometry determined by the DFT calculations is used the best agreement is obtained when $P_{iso}(\phi_{23,24})$ is essentially a delta function ($h_{23,24}=0$) located at ϕ_{min}(C23–C24)=90°. This indicates that the geometry also needs to be changed, and varying the angles $\theta_{29,23,5}=\theta_{30,23,5}$, keeping $h_{23,24}=0$, and ϕ_{min}(C23–C24)=90° improves the fitting of calculated to observed values of the residual dipolar couplings. A delta function is not a realistic form for $P_{iso}(\phi_{23,24})$, and changing this to a Gaussian with a finite width leads to the values of $\theta_{29,23,5}=\theta_{30,23,5}=111.2\pm0.2°$ to $111.8\pm0.2°$ when $h_{23,24}$ is fixed at 5–20 Hz.

The conformation of the alkyl chain

The conformational probability distribution, $P_{LC}^{chain}(n)$, has already been predicted by comparing observed and calculated residual quadrupolar splittings, and now this distribution is derived using the residual dipolar couplings between ^{13}C and ^{1}H nuclei in the aliphatic chain. The increased data set allows the bond rotational probability distributions, in the alkyl chain to be investigated independently. To do this the chain is divided into rigid fragments defined by three carbon atoms, $C_{j\text{-}1}$, C_j and C_k, as shown in Figure 9.

The residual dipolar couplings between nuclei in the group of atoms in the fragment defined by carbon atoms $C_{j\text{-}1}$, C_j, C_k and C_{k+1} are then used to investigate the rotational probability distributions, $P_{LC}(\phi_{jk})$ and $P_{iso}(\phi_{jk})$, about the bond, C_j–C_k.

The bond-rotational probability distributions $P_{LC}(\phi_{23,24})$ and $P_{iso}(\phi_{23,24})$

The fragment **2** is considered in which C25, H30 and H_{31} rotate through an angle $\phi_{23,24}$ relative to the rigid fragment **1**. The experiment values of D_{CH} that are obtained for this rigid fragment **1** are $D_{23,29}=D_{23,30}$, $D_{5,28}=D_{5,29}$ and $D_{24,28}=D_{24,29}$. The C5–C23 bond is part of the biphenyl group, and so the value of $D_{5,23}$ can be predicted from the analysis of the couplings within the biphenyl group. Note that this interconnection between molecular fragments is a common feature of the analyses of all the relative chain segment rotations. The symmetry of fragment **1** is C_S and hence three independent local order parameters are required in the calculation of dipolar couplings within the group. This translates into three axially-symmetric interaction parameters, $\varepsilon_{r,s}(2)$, for this first chain fragment pointing along directions specified by atoms r and s, and these were chosen to be $\varepsilon_{5,23}(2)$, $\varepsilon_{23,28}(2)=\varepsilon_{23,29}(2)$ and $\varepsilon_{28,29}(2)$. Note that these are labelled with the index 2 since they are used when considering rotation about the bond C23–C24. A fourth interaction tensor, $\varepsilon_{23,25}(2)$, was added to allow for the dependence of the local order tensor on the rotation of the atoms C24, C25, H30 and H31 in fragment **2**. The bond rotational probability distribution $P_{iso}(\phi_{23,24})$ was represented in the same way as for

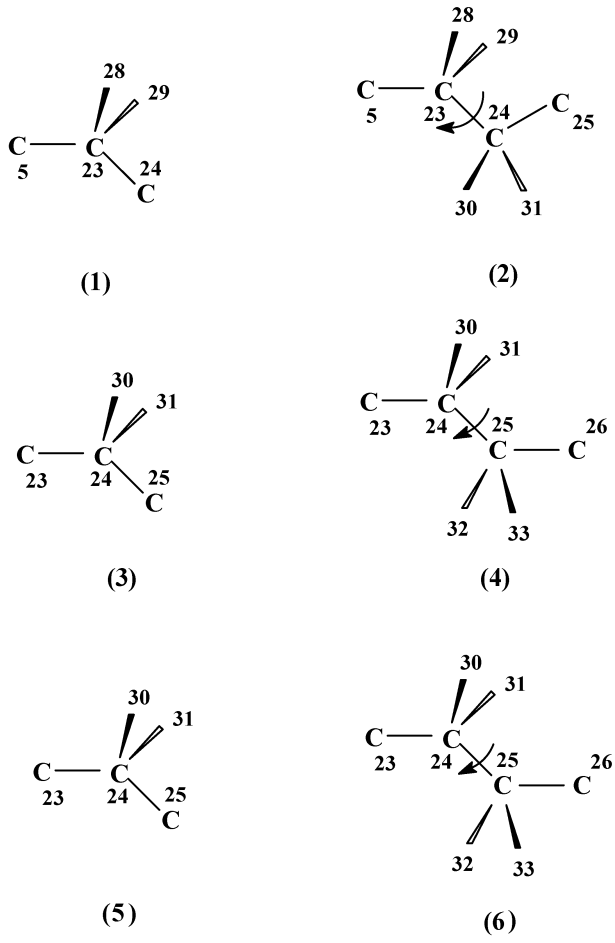

Figure 9. The chain fragments.

the rotation about the inter-ring bond, but now involving three gaussian functions:

$$P_{iso}^{j,k}(\phi) = \frac{A(j,k)}{\left(2\pi h_t^2\right)^{\frac{1}{2}}} \exp\left[-\frac{\left(\phi - 180^0\right)^2}{2h_t^2}\right] + \frac{\frac{1}{2}(1-A(j,k)}{\left(2\pi h_g^2\right)^{\frac{1}{2}}} \left\{ \exp\left[-\frac{\left(\phi - 180^0 + \phi_g\right)^2}{2h_g^2}\right] + \exp\left[-\frac{\left(\phi - 180^0 - \phi_g\right)^2}{2h_g^2}\right] - \right\}, \quad (27)$$

centred on the trans (ϕ=180°) and the two gauche positions at 180°−ϕ_g=66° and 180°+ϕ_g=294°, as predicted by the B3LYP/6-311G** calculations.

There are seven unknowns, $\varepsilon_{5,23}(2)$, $\varepsilon_{23,28}(2)$=$\varepsilon_{23,29}(2)$, $\varepsilon_{28,29}(2)$, $\varepsilon_{23,25}(2)$, $A(23,24)$, h_t and h_g, to be matched to seven dipolar couplings. The unknowns were reduced by setting h_t=h_g, but varying all these parameters did not lead to well-defined values of the six variables. However, this problem was removed by setting h_t=h_g=15°. It was now found possible to add the angles $\theta_{5,23,28}$=$\theta_{5,23,29}$ to the variables and to obtain the results shown in Table 8.

The two probability functions $P_{iso}(\phi_{23,24})$ and $P_{LC}(\phi_{23,24})$ obtained are shown in Figure 10. The percentage in the *trans* form, as measured by the area from $\phi_{23,24}$=120 to 240°, is 77% in the nematic as opposed to 65% in the isotropic phase.

Table 8. The bond angles $\theta_{5,23,28}$=$\theta_{5,23,29}$, local, fragment interaction parameters, $\varepsilon_{j,k}(2)$/RT for chain fragment **2**, and the weighting factor, $A(23,24)$ for the Gaussian functions in the probability $P_{iso}(\phi_{23,24})$ for rotation about the bond C23–C24 through an angle $\phi_{23,24}$.

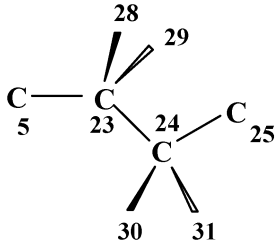

$\theta_{5,23,28}$=$\theta_{5,23,29}$=110.6±0.4°
$\varepsilon_{5,23}(2)/RT$=2.6±0.1
($\varepsilon_{23,28}(2)$=$\varepsilon_{23,29}(2)$)/RT=0.3±0.4
$\varepsilon_{28,29}(2)/RT$=−0.5±0.3
$\varepsilon_{23,25}(2)/RT$=1.1±0.4
$A(23,24)$=0.65±0.09

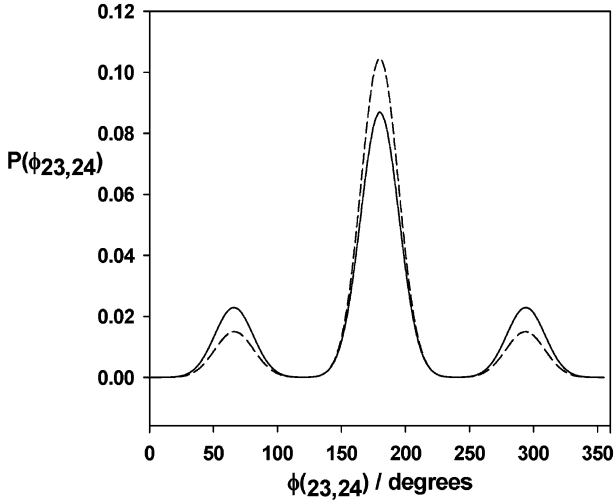

Figure 10. The probabilities $P_{iso}(\phi_{23,24})$ (full line) and $P_{LC}(\phi_{23,24})$ (dashed line) determined for rotation about the bond C23–C24 in 5CB.

The bond-rotational probability distributions $P_{LC}(\phi_{24,25})$ and $P_{iso}(\phi_{24,25})$

The next fragment in the chain, **3**, shares atoms 23, 24, 25, 30 and 31 with fragment **2**, and predicted values of $D_{23,24}$, $D_{24,25}$ and $D_{30,31}$ can be used, together with measured values of $D_{23,30}$=$D_{23,31}$, $D_{24,30}$=$D_{24,31}$ and $D_{25,30}$=$D_{25,31}$, to determine the local order matrix for this fragment. Rotating the group C26H32H33 about the bond C24–C25 averages the couplings $D_{26,30}$=$D_{26,31}$, $D_{25,32}$=$D_{25,33}$ and $D_{26,32}$=$D_{26,33}$ in fragment **4**.

The fragment interaction parameters used were $\varepsilon_{25,26}(4)$, $\varepsilon_{25,31}(4)$=$\varepsilon_{25,32}(4)$, and $\varepsilon_{25,27}(4)$ and their optimized values, together with the value determined for $A(24,25)$ are given in Table 9.

The probability functions $P_{LC}(\phi_{24,25})$ and $P_{iso}(\phi_{24,25})$ are shown in Figure 11, where it is seen that they practically coincide, and in both cases there is 62% of the *trans* form present. This equality reflects the relatively low local order of this fragment.

The bond-rotational probability distributions $P_{LC}(\phi_{25,26})$ and $P_{iso}(\phi_{25,26})$

The methyl group is assumed to rotate about a threefold axis along C26–C27 with a barrier to rotation sufficiently high that only the three equivalent minimum energy structures need to be averaged. With these assumptions the average value, $D_{k\mathrm{H}}$, of the residual dipolar couplings involving the methyl protons is given by

$$D_{k\mathrm{H}} = \frac{1}{3}[D_{k36} + D_{k37} + D_{k38}]. \quad (28)$$

Table 9. The local, fragment interaction parameters, $\varepsilon_{j,k}(4)/RT$ for chain fragment **4**, and the weighting factor, $A(24,25)$ for the Gaussian functions in the probability $P_{iso}(\phi_{24,25})$ for rotation about the bond C24–C25 through an angle $\phi_{24,25}$.

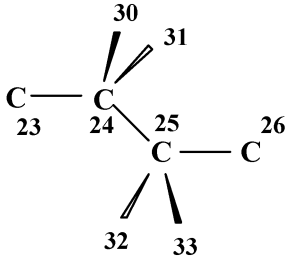

$\varepsilon_{24,25}(4)/RT$	1.84 ± 0.2
$\varepsilon_{24,30}(4)/RT$	-0.64 ± 0.06
$\varepsilon_{24,26}(4)/RT$	0.40 ± 0.01
$\varepsilon_{30,31}(4)/RT$	1.04 ± 0.04
$A(24,25)$	0.62 ± 0.07

The methyl group therefore can be considered to be fixed in one minimum energy conformation, and rotation about the bond C25–C26 involves relative movement of two rigid fragments **5** and **6**.

Residual dipolar couplings $D_{24,25}$ and $D_{32,33}$ are predicted from the analysis of rotation involving fragment **4** and are used together with the experimental values of $D_{24,32}=D_{24,33}$, $D_{25,32}=D_{25,33}$ and $D_{26,32}=D_{26,33}$ to investigate the structure and local order parameters for fragment **5**. Three fragment interaction parameters are required to determine the local order for this fragment with symmetry C_S, and varying these with the geometry fixed at that calculated by B3LYP/6-311G**, but varying $r_{25,32}=r_{25,33}$ produces almost exact agreement between the above five couplings and those calculated. The calculations on fragment **4** are used to

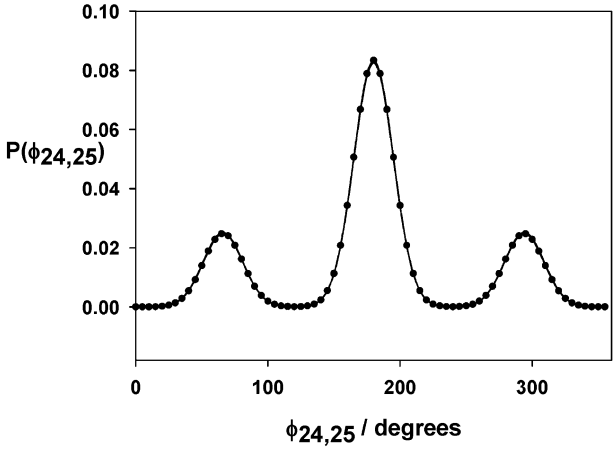

Figure 11. The probabilities $P_{iso}(\phi_{24,25})$ (full line) and $P_{LC}(\phi_{24,25})$ (•) determined for rotation about the bond C24–C25 in 5CB.

predict a value for $D_{25,26}$, which is used to together with the set:

$$D_{25,34} = D_{25,35};$$
$$D_{25,36} = D_{25,37} = D_{25,38},;$$
$$D_{26,34} = D_{26,35};$$
$$D_{26,36} = D_{26,37} = D_{26,38};$$
$$D_{27,34} = D_{27,35};$$
$$D_{27,36} = D_{27,37} = D_{27,38},$$

to investigate the local order and structure of fragment **6**. Three local interaction tensor components are necessary to specify the local order, and varying just these with the geometry fixed at that calculated by the B3LYP/6-311G** method leads to close but not perfect agreement between observed and calculated dipolar couplings, but these could be brought into exact agreement by varying also the C–H bond lengths $r_{26,34}=r_{26,35}$, $r_{27,36}=r_{26,37}=r_{27,38}$ and the angle $\theta_{25,26,27}$ to give the results shown in Table 10. Note that the unusually long bond lengths found, and the large change in the bond angle are probably a consequence of not averaging the residual dipolar couplings over vibrational motion.

Table 10. The optimized values of bond lengths $r_{25,32}=r_{25,33}$, $r_{26,34}=r_{26,35}$ and $r_{27,36}=r_{27,37}=r_{27,38}$ (Å) the angle $\theta_{25,26,27}$ (°), and the local, fragment interaction parameters, $\varepsilon_{j,k}(6)/RT$ for chain fragment **6**, and the weighting factor, $A(25,26)$ for the Gaussian functions with the width fixed at 15° in the probability $P_{iso}(\phi_{25,26})$ for rotation about the bond C25–C26 through an angle $\phi_{25,26}$.

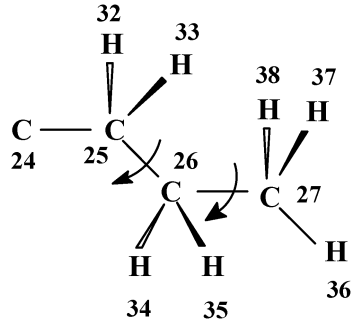

$r_{25,32}=r_{25,33}$	1.088 ± 0.001
$r_{26,34}=r_{26,35}$	1.11
$r_{27,36}=r_{27,37}=r_{27,38}$	1.13
$\theta_{25,26,27}$	106.1
$\varepsilon_{25,26}(6)/RT$	1.112 ± 0.005
$\varepsilon_{25,27}(6)/RT$	0.808 ± 0.003
$\varepsilon_{33,34}(6)/RT$	0.072 ± 0.005
$\varepsilon_{27,28}(6)/RT$	0.885 ± 0.009
$A(25,26)$	0.597 ± 0.005

The rotation of fragment **6** relative to **5** about the C25–C26 bond was then investigated using the two sets of dipolar couplings used to investigate the rigid fragments, plus the inter-fragment couplings $D_{26,32}=D_{26,33}$. It was found that varying the four local interaction parameters $\varepsilon_{25,26}(6)$, $\varepsilon_{25,27}(6)$, $\varepsilon_{33,34}(6)$, and $\varepsilon_{27,28}(6)$ and the intensity factor $A(25,26)$ produced good agreement between observed and calculated dipolar couplings with the results shown in Table 11. Varying also the width, h, of the gaussian functions did not lead to stable iterations, and so a fixed value of 15° was used. Changing this value from 10 to 20° varies the term $A(26,27)$ by <0.01.

The probability distributions are shown in Figure 12.

The fraction of the trans form, defined as the area between 120° and 240°, increases from 60% in the isotropic phase to 0.69% in the nematic.

7. Conclusions

Both 1D deuterium and the 2D carbon PDLF NMR experiments can now produce good quality spectra on un-enriched samples of liquid crystals, and this has been demonstrated here with the example of the nematogen 5CB. The deuterium spectrum obtained contains a relatively limited amount of useful information, and its main use will be to complement the much larger data set obtained from the ^{13}C PDLF experiment. The latter is very rich in information on the structure, conformation and orientational order of the molecules, and should be the method of choice for investigating these properties. In particular, it has been demonstrated for 5CB that the bond rotational probability distributions can be investigated separately for each bond in the molecule. This is done by considering the relative conformations of small submolecular fragments, such as the biphenyl group and segments of the alkyl chain. In contrast, the residual deuterium quadrupolar splittings obtained for each set of equivalent deuteriums in 5CB can be used only to test simplified models for the conformational distributions of the whole alkyl chain. This limits the length of chain which can be studied via deuterium NMR since the number of conformations even in the simple RIS model is 3^{N-2}, where N is the number of chain segments. For molecules with a single chain the limit is about $N=10$, whereas for two or more chains a limit is reached with for quite short alkyl chains. The chain length limit for the ^{13}C PDLF experiment is determined only by the spectral resolution, which may become a problem as the number of resonances separated by small chemical shifts increases. This limit will recede as the field strength of NMR spectrometers increases.

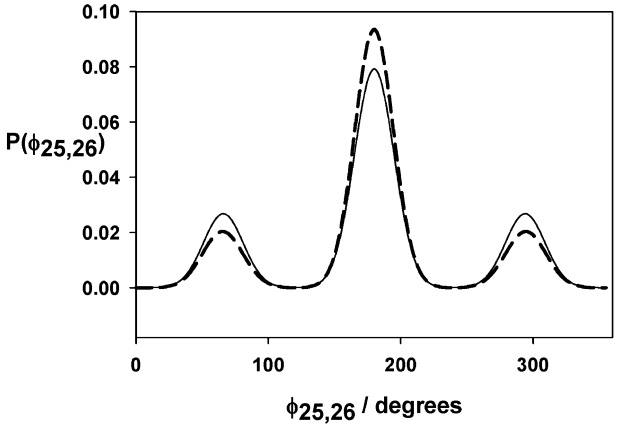

Figure 12. The probability distributions $P_{LC}(\phi_{25,26})$ (dashed line) and $P_{iso}(\phi_{25,26})$ (continuous line) for rotation about the bond C25–C26 in 5CB.

The observed residual quadrupolar splittings and residual dipolar couplings are averages over small-amplitude vibrational motion. There are no theoretical models yet in place for averaging the residual quadrupolar splittings, and such an effect is usually neglected. It is possible to calculate the effect of vibrational motion on residual dipolar couplings between nuclei in rigid molecules, and approximate methods have been proposed for flexible, small molecules (*48, 49*). However, a practical procedure for molecules containing multiple bond rotations awaits development.

It has been demonstrated here that deuterium spectra of strongly ordered molecules, such as 5CB in the nematic phase, yield much less information that the ^{13}C PDLF experiment. But, this is not the case for weakly ordered solutes dissolved in liquid crystalline solvents. In this case the deuterium spectra are easily obtained, particularly by using a cryoprobe tuned to deuterium, whilst obtaining well-resolved ^{13}C PDLF spectra on such solutions has yet to be demonstrated.

Acknowledgment

This work is supported in part by a grant from PRIN 2005 (Italian MUIR).

References

(1) Rowell J.C.; Phillips W.D.; Melby L.R.; Panar M. *J. Chem. Phys.* **1965**, *43*, 3442–3454.
(2) Emsley J.W. (Ed.), *NMR of Liquid Crystals*; Dordrecht: Riedel, 1985.
(3) Dong R.Y. *Nuclear Magnetic Resonance of Liquid Crystals*; Springer-Verlag: Berlin, 1994.
(4) Vold R.R., In *NMR of Liquid Crystals*; Emsley J.W. (Ed.), Dordrecht: Riedel, 1985, Chapter 11.

(5) Beckman P.A.; Emsley J.W.; Luckhurst G.R.; Turner D.L. *Mol. Phys.* **1983**, *50*, 699–725.
(6) Beckman P.A.; Emsley J.W.; Luckhurst G.R.; Turner D.L. *Mol. Phys.* **1986**, *59*, 97–125.
(7) Fung B.M.; Afzal J.; Foss T.L.; Chau M.H. *J. Chem. Phys. A* **1986**, *85*, 4808–4814.
(8) Fung B.M., In *Encyclopaedia of NMR*; Grant D.M., Harris R.K. (Eds), John Wiley & Sons: Chichester, 1996. pp. 2744.
(9) Hong M.; Pines A.; Calderelli S. *J. Phys. Chem. A* **1996**, *100*, 14815–14822.
(10) Calderelli S.; Hong M.; Emsley L.; Pines A. *J. Phys. Chem. A* **1996**, *100*, 18696–18701.
(11) Tabayashi K.; Akasaka K. *J. Phys. Chem. B* **1997**, *101*, 5108–5111.
(12) Sakellariou D.; Lesage A.; Hodgkinson P.; Emsley L. *Chem. Phys. Lett.* **2000**, *319*, 253–260.
(13) Fung B.M.; Khitrin A.K.; Ermolaev K. *J. Magn. Resonance* **2000**, *142*, 97–101.
(14) States D.J.; Haberkorn R.A.; Ruben D.J. *J. Magn. Resonance* **1982**, *48*, 286–292.
(15) Lesot P.; Merlet D.; Loewenstein A.; Courtieu J. *Tetrahedron: Asymmetry* **1998**, *9*, 1871–1881.
(16) Sarfati M.; Lesot P.; Merlet D.; Courtieu J. *Chem. Commun.* **2000**, 2069–2091 and references therein.
(17) Lesot P.; Sarfati M.; Courtieu J. *Chem. Eur. J.* **2003**, *9*, 1724–1745.
(18) Kovacs H.; Moskau D.; Spraul M. *Prog. NMR Spectrosc.* **2005**, *45*, 131–155.
(19) Emsley J.W.; Lesot P.; Courtieu J.; Merlet D. *Phys. Chem. Chem. Phys.* **2004**, *6*, 5331–5337.
(20) *Gaussian* 03, revision C.02; Gaussian Inc: Wallingford, CT, 2004.
(21) Emsley J.W.; De Luca G.; Lesage A.; Merlet D.; Pileio G. *Liq. Cryst.* **2007**, *34*, 1071–1093.
(22) Emsley J.W.; Luckhurst G.R.; Stockley C.P. *Mol. Phys.* **1981**, *44*, 565–580.
(23) Emsley J.W.; Luckhurst G.R.; Stockley C.P. *Proc. R. Soc. A* **1982**, *381*, 117–138.
(24) Brink D.M.; Satchler G.R. *Angular Momentum,* 2nd ed., Oxford University Press: Oxford, 1968.
(25) Fung B.M.; Ermolaev K.; Yu Y. *J. Magn. Resonance* **1999**, *138*, 28–35.
(26) Celebre G.; De Luca G.; Longeri M.; Sicilia E. *J. chem. Inf. Comput. Sci.* **1994**, *34*, 539–545.
(27) Jokisaari J.; Kounanoja J.; Pulkkinen A.; Vaananen T. *Mol. Phys.* **1981**, *44*, 197–208.
(28) Wray V.; Ernst L.; Lusting E. *J. Magn. Resonance* **1977**, *27*, 1–21.
(29) Merlet D.; Lesage A.; Emsley J.W. *J. Phys. Chem. A* **2005**, *109*, 5070–5078.
(30) Auger C.; Lesage A.; Caldarelli S.; Hodgkinson P.; Emsley L. *J. Am. Chem. Soc.* **1997**, *119*, 12000–12001.
(31) Auger C.; Lesage A.; Caldarelli S.; Hodgkinson P.; Emsley L. *J. Phys. Chem. B* **1998**, *102*, 3718–3723.
(32) Courtieu J.; Bayle J.-P.; Fung B.M. *Prog. NMR Spectrosc.* **1994**, *26*, 141–169.
(33) Edgar M.; Emsley J.W.; Furby M.I.C. *J. Magn. Resonance* **1997**, *128*, 105–113.
(34) Ciampi E.; Furby M.I.C.; Brennan L.; Emsley J.W.; Lesage A.; Emsley L. *Liq. Cryst.* **1999**, *26*, 109–125.
(35) Ziani L.; Courtieu J.; Merlet D. *J. Magn. Resonance* **2006**, *183*, 60–67.
(36) Farjon J.; Baltaze J.P.; Lesot P.; Merlet D.; Courtieu J. *Magn. Resonance Chem.* **2004**, *42*, 594–599.
(37) Deng W.; Cheeseman J.R.; Frisch M.J. *J. Chem. Theory Computation* **2006**, *2*, 1028–1037.
(38) Celebre G.; De Luca G.; Emsley J.W.; Foord E.K.; Longeri M.; Lucchesini F.; Pileio G. *J. Chem. Phys.* **2003**, *118*, 6417–6426.
(39) Emsley J.W. *Phys. Chem. Chem. Phys.* **2006**, *8*, 3726–3731.
(40) Celebre G.; Longeri M.; Sicilia E.; Emsley J.W. *Liq. Cryst.* **1990**, *7*, 731–737.
(41) Sinton S.W.; Zax D.B.; Murdoch J.B.; Pines A. *Mol. Phys.* **1984**, *53*, 333–362.
(42) Lucas N.J.D. *Mol. Phys.* **1971**, *22*, 147–154.
(43) Lucas N.J.D. *Mol. Phys.* **1971**, *22*, 233–239.
(44) Lucas N.J.D. *Mol. Phys.* **1972**, *23*, 825–826.
(45) Lesot P.; Merlet D.; Courtieu J.; Emsley J.W.; Rantala T.T.; Jokisaari J. *J. Phys. Chem. A* **1997**, *101*, 5719–5724.
(46) Celebre G.; De Luca G.; Longeri M.; Pileio G. *Mol. Cryst. Liq. Cryst.* **2007**, *465*, 289–299.
(47) Hanemann T.; Haase W.; Svoboda I.; Fuess H. *Liq. Cryst.* **1995**, *19*, 699–702.
(48) Concistré M.; De Lorenzo L.; De Luca G.; Longeri M.; Pileio G.; Raos G. *J. Phys. Chem. A* **2005**, *109*, 9953–9963.
(49) Celebre G.; Concistré M.; De Luca G.; Longeri M.; Pileio G.; Emsley J.W. *Chem. Eur.* **2005**, *11*, 3599–3608.